Oscillation Mechanics of the body

A new application in endoscopic surgery

by

F. Sterke

to obtain the degree of Master of Science
Delft University of Technology,

Student number:	1512404	
Supervisors:	Dr. ir. A. C. Schouten,	TU Delft
	Ir. T. G. Goos,	Erasmus MC
	Drs. W. van Weteringen	Erasmus MC

This thesis is confidential and cannot be made public until Februari, 2023.

TU Delft

List of abbreviations

Abbreviaton	**Description**
Forced pressure oscillations	Pressure oscillations imposed by an external source.
FOT	Forced Oscillation Technique.
IAP	Intra abdominal pressure, the pressure within the surgical working space.
Impedance	The complex ratio between pressure and flow as a function of frequency.
Insufflation	Inflating a body cavity with gas.
Insufflator	Device used for insufflation of the pneumoperitoneum.
Minimal access surgery	A surgical technique that uses small incisions to enter the surgical site.
Pneumoperitoneum	An abnormal bubble of gas within the body.
Reactance	The reactive component of impedance related to energy storage.
Resistance	The resistive component of impedance related to the dissipation of energy.
R_{ws}	Resistance component of surgical working space impedance.
Trocar	A hollow tube used to insert gas or surgical tools into the surgical site.
X_{ws}	Reactive component of surgical working space impedance.
Z_{ws}	Surgical working space impedance.

Contents

1

Oscillation Mechanics of the surgical working space

Author: F. Sterke
Erasmus MC Sophia and Delft University of Technology
Department of Pediatrics, Department of Pediatric Surgery, Department of Biomedical Engineering

Abstract: In minimal access surgery, the creation of a large surgical working space facilitates the surgeon and shortens the duration of surgical procedures. Using a high intra abdominal pressure to increase the surgical workspace could damage the surrounding tissue due to overdistension. Surgical working space compliance describes the relation between the volumetric gain rate of surgical working space and the pressure used. The forced oscillation technique could enable monitoring of the surgical working space compliance to prevent overdistension, without prolonging the surgical procedure. Endoscopic forced oscillations have been applied in a porcine model. Frequency and pressure sweeps have been performed to investigate if this technique can be used to monitor surgical working space compliance. Using 6 Hz forced pressure oscillations with a peak-to-peak amplitude of 2hPa amplitude can be used to monitor changes in surgical working space compliance. This technique seems safe for the subjects and can be used to prevent overdistension and could enable closed-loop controlled insufflation of the surgical working space.

Keywords: Minimal Access Surgery· laparoscopy · thoracoscopy · working space · compliance · forced oscillations technique.

1. Introduction

In minimal access surgery, the surgeon uses small incisions to enter the surgical site. Minimal access surgery has shown to be advantageous over conventional surgery because it reduces the chance of infection, amount of postoperative pain and results in less scar tissue. Within the body there is no physiological space for the surgery, yet space can be created by insufflating a pressurized gas. A pneumoperitoneum is created by insufflating carbon dioxide gas through a trocar into the surgical site. The surgical working space is commonly defined as the volume of the pneumoperitoneum.
A large surgical working space facilitates the surgeon and shortens the duration of surgical procedures. Shortening the procedure improves medical safety and reduces the amount of postoperative pain [12]. This working space can be enlarged by increasing the pressure with which the carbon dioxide gas is insufflated..
Using high pressures for creating surgical working space can have adverse effects. Firstly, additional carbon dioxide diffuses into the bloodvessels surrounding the surgical working space. Imposing a load onto the respiratory system requires adjustment of the mechanical ventilator settings. Secondly, organ perfusion is reduced when subjected to high internal pressure levels. For example, lung collapse will occur when the mechanical ventilator settings are not adjusted accordingly. Thirdly, the tissues surrounding the surgical working space get damaged due to overdistension.

1.1. Surgical working space compliance

The relation between the pressure used for insufflation and the created surgical working space is de-

scribed by a compliance curve. Vlot et al. [10] have experimentely determined compliance curves in pigs , figure 1.1. The steepness of this curve is the surgical working space compliance, $C_{ws} = \Delta V / \Delta p$. The surgical working space gain per pressure increment is influenced by body size, tissue condition(aging) and affected by muscle activity(neuromuscular blockade). Tissue surrounding the surgical working space stiffens when it is overdistended, reducing the surgical working space compliance. If the surgeon could be informed about working space compliance, he or she can make an adequate decision on the requirement of additional space, even when it will lead to overdistension of the tissue. This study was done to check whether the forced oscillation technique can be used for identifying changes in surgical working space compliance. The main goal is to prevent overdistension of the surrounding tissues. In the future this information on the surgical working space compliance could aid in the automated control of insufflation.

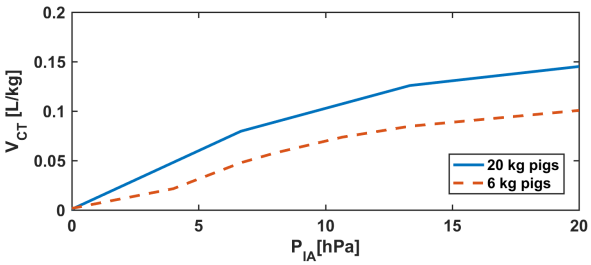

Figure 1.1: The effect of body size onto static working space compliance in a porcine model, 6kg pigs and 20kg pigs, base on data obtained by Vlot et al. [11]

Ideally the insufflation device would measure the volume and pressure to present the patient-specific compliance curve to the surgeon. Unfortunately, leakage of carbon dioxide inhibits estimation of the created volume by integrating the volumetric flow rate. Therefore reliable volumetric measurements are difficult to obtain without prolonging the surgical procedure. The lack of information on the volume of the surgical working space deters continuous monitoring of surgical working space compliance.

1.2. Surgical working space impedance

A solution to continuously monitor the surgical working space compliance might be found in a technique used for estimating respiratory impedance. This so called forced oscillation technique (FOT) was first described by DuBois et al. [3] in 1956. Small forced pressure oscillations around a constant pressure are used to determine the mechanical compliance of the lungs [9]. Currently this technique is being used to diagnose pulmonary diseases [4].

Mechanical impedance is defined as the amount of pressure needed to create flow, $Z(\omega) = p(\omega)/\dot{V}(\omega)$, [5]. The surgical working space impedance, Z_{ws}, could be determined by measuring the pressure and flow at the trocar, this gives equation 1.1. A reduction in compliance will increase the impedance, more pressure is needed to create the same flow. The whole detection method is based on the electrical analogy of a resistor(R), capacitance(C) and inductor(L) in series. Pressure would equal voltage and flow would equal current. In the pneumatic domain the Z_{ws} could be modeled as a balloon being inflated, see figure 1.2 for clarification. Changes in the capacitive properties of the system would indicate a change in surgical working space compliance.

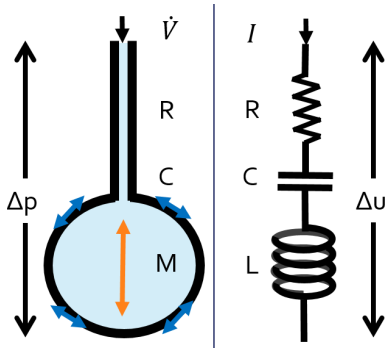

Figure 1.2: Analogy between the pneumatic and electrical domain, $Z = p/\dot{V} = U/I$. In both cases R equals resistance. Surgical working space compliance can be described by an capacity. The mass(M) of the gas in the working space can be described by an inductor(L).

The frequency behaviour of the input impedance Z_{ws} can be decomposed into resistance,R_{ws}, and reactance, X_{ws}. Reactance itself can also be decomposed, at low frequencies the capacitance will dominate the impedance behaviour, equation 1.3. At the resonance frequency the reactance becomes zero, therefore the impedance behaviour will be dominated by the resistance. At higher frequencies the reactance will become more positive and the behaviour is dominated by the inertial properties of the system.

$$Z_{ws}(\omega) = \frac{P_{\text{trocar}}(\omega)}{\dot{V}_{\text{trocar}}(\omega)} \tag{1.1}$$

$$Z_{ws}(\omega) = R_{ws}(\omega) + i \cdot X_{ws}(\omega) \tag{1.2}$$

$$X_{ws}(\omega) = \omega \cdot L - \frac{1}{\omega \cdot C} \tag{1.3}$$

This study was done to check whether the forced oscillation technique can be used for identifying changes in surgical working space compliance. The main goal is to prevent overdistension of the surrounding tissues. In the future this information on

the surgical working space compliance could aid in the automated control of insufflation. Based on an impedance model of a balloon it was hypothesized that low frequency forced oscillations can be used to monitor surgical workspace compliance. Therefore the first objective was to identify the oscillatory mechanics of the surgical working space. The second objective was to determine how the impedance behaves if the mean insufflation pressure is increased.

2. Methods

2.1. Subjects

Ethical approval was obtained from the institutional ethics committee. Three in-vivo experiments were done in female Yorkshire pigs. All subjects received anesthetics and muscle relaxants. Respiratory support was provided using a mechanical ventilator. The ventilator settings were adjusted to provide sufficient oxygen delivery and carbon dioxide elimination, using the pressure control mode. A trocar was put in place for carbon dioxide insufflation. An intra-abdominal pressure (IAP) of 5 hPa was applied. The creation of the pneumoperitoneum was verified using an endoscope.

2.2. Forced Oscillations

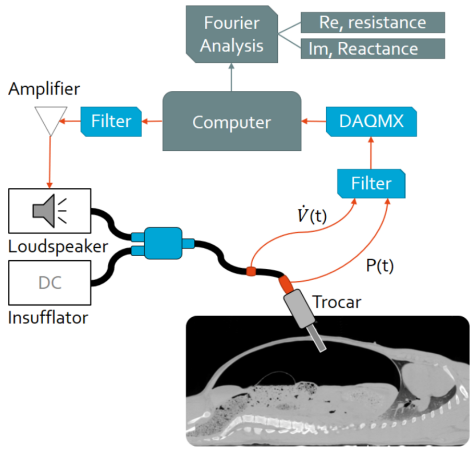

Figure 1.3: Endoscopic FOT setup for surgical working space impedance measurements. The insufflation pressure (p_{troc}) and flow ($\dot{V}_{troc}$) are measured close to the trocar.

The 3.5 mm audio jack of the computer was used to generate the forced oscillations. A speaker (TS-W261D4 Pioneer, Honkomagome, Japan) and power amplifier (VLP1500, American Audio, Los Angeles, CA, USA) were used to create the forced pressure oscillations. This amplifier has a built-in low pass filter with a 200 Hz cutoff frequency. The speaker was connected to a 4 L conical piece to convert the pressure into a 19 mm hose. A custom-built manifold was used to combine the mean pressure from the insufflator (Endoflator 40, Karl Storz, Tuttlingen, Germany) with the forced pressure signal from the speaker. The manifold was connected to a regular insufflation tubing set with a gas filter. A 50 hPa pressure release valve (AV319, Wittgas, Witten, Germany) was connected to the manifold for medical safety. Figure 1.3 shows the schematic layout of this endoscopic FOT setup. The setup was designed using guidelines and literature available for pulmonary FOT, [2, 8], more details can be found in appendix A.

2.3. Protocol

Information on oscillatory behaviour of the subject's surgical working space was be obtained through applying frequency sweeps. During these frequency sweeps, the mean IAP was kept constant. To compare between subjects, at least one frequency sweep was done at 10 hPa mean IAP. The frequency sweep was executed stepwise. The response to every frequency between 4-20 Hz was recorded for 60 [s]. Before every step the forced pressure amplitude was adjusted to 2 hPa peak-to-peak. Similar peak-to-peak pressures are used in pulmonary FOT, [8]. In subjects 2 and 3 an additional frequency sweep was done at a mean IAP of 5 hPa.

Changes in surgical working space impedance were investigated by applying pressure sweeps. During these sweeps the forced pressure signal was kept constant. The frequency used was 6 Hz and the amplitude was kept at 2 hPa peak-to-peak. The 6 Hz frequency was chosen based on a previous experiment in a post-mortem subject. The mean IAP pressure setting was increased stepwise from 1-20 hPa. At each pressure step the forced pressure signal was applied for 60 [s]. Between every step there was time for the insufflator to reach the mean target pressure. In some subjects multiple pressure sweeps were done. After each pressure sweep the pneumoperitoneum was deflated. The subject was given a pause to eliminate the excess carbon dioxide and restore oxygenation levels.

2.4. Measurements

During the sine and pressure sweeps the trocar pressure (p_{troc}) and flow ($\dot{V}_{troc}$) were measured at the gas intake port of a modified trocar (VersaStep, Covidien, Dublin, Ireland). Additional pressure measurements were performed at the manifold. Four pressure transducers (HCS160MD, Honeywell, Morris Plains, New Jersey, USA) calibrated up to 160 hPa were used. Two transducers were used for differential flow pressure measurements in a fixed orifice flow sensor (Neonatal flow sensor, Respironics Inc, Murrysville, PA, United States). This sensor has been calibrated for carbon dioxide up to 20 [L/min]. To prevent aliasing all electrical signals were filtered using a analog low-pass filter(f_{cuttof}= 100 Hz), and

sampled at 1000 Hz by a an analogue-to-digital converter (DAQMX 6211, National Instruments, Austin, TX, USA). In Labview the signals were digitally low-pass filtered(f_{cuttof}= 30 Hz) and re-sampled at 200 Hz for storage and computational analysis.

2.5. Data Analysis

Matlab was used for analyzing the data. All samples were band-pass filtered ±1 Hz around the forced signal frequency used for that sample. After this the samples were divided into 5 second samples and a Hanning-window was applied. A Fourier analysis was used to determine the resistance and reactance.
In both cases Welch averaging has been applied. Frequency sweep samples were averaged per forced signal frequency. Pressure sweeps were averaged per level of mean IAP. For all sweeps the coefficient of variation, μ/σ, was calculated for the resistance and reactance. The mean, μ, was taken from the Welch averaging. For calculation of the standard deviation, σ, the amount of variation between the separate 5 second time samples was used.
The impedance behaviour of the flow sensor depends on the mean IAP and forced signal frequency used. The calculations were corrected for this behaviour.
Correction factors were calculated from measurements on a reference impedance, whose theoretical impedance could be determined. The calibration procedure is described in appendix A.

3. Results

3.1. Subjects

For sedation, the first two in-vivo subjects were administered Rocuronium, Midazolam, Sufentanil and Ketamine, all intravenously. Iso-flurane was used used to sedate subject 4. This type of anesthesia is administered through inhalation. A preliminary experiment was done in a postmortem 65[kg] pig without any ventilation, all results can be found in appendix D. The physical characteristics and mechanical ventilator settings of all in-vivo experiments are given in table 1.1.

3.2. Forced pressure signal

In figure 1.4 the result after combining the DC and AC pressure signal is shown. The forced pressure signal dampens throughout the system. At the manifold the peak-to-peak amplitude is larger than 20 hPa. An amplitude reduction is caused by the insufflation tube and sensor. Harmonic distortions are present, these harmonics can be seen in the spectral density plot. The second harmonic has roughly the same amplitude. In this sample the mean pressure at the trocar is 0.9 hPa lower than the target pressure 10 hPa. The code used for analysing the data is added in B.

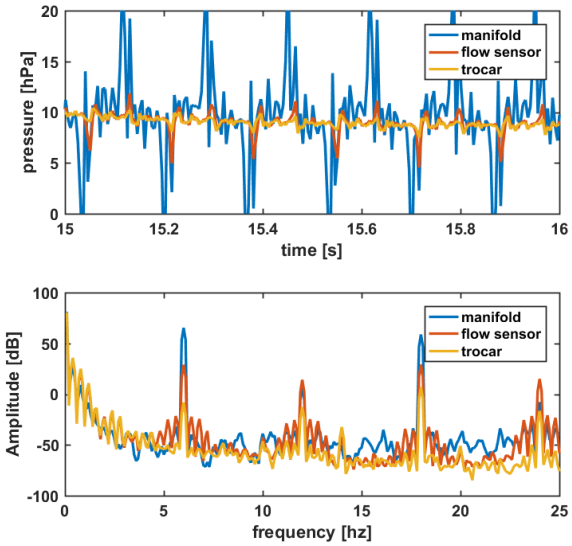

Figure 1.4: Time sample in subject 3. Recorded pressure at manifold, pressure at the manifold side of the flow sensor and pressure at the trocar. The forced pressure signal frequency was set to 6 Hz, mean IAP was set to 10 hPa

3.3. Frequency sweeps

The results of the performed frequency sweeps are shown in figure 1.5. In subject 3 an additional frequency sweep was done at a mean IAP of 5 hPa. In subjects 2 and 3, the reactance behaves similar to the model in equation 1.3. It increases when the frequency increases. It was expected that the reactance would become positive within the measured frequency range. The resonance frequency seems to be outside the measurement window. The results obtained in subject 3 at a mean IAP of 5 hPa and 10 hPa are similar. The resistance is higher at low frequencies, the reactance behaves the same.

No.	Weight [kg]	IAP hPa	p_{EEP} hPa	p_{IP} hPa	V_{tidal}(L)	T_{resp}([s])	I:E [-]	Anesthetic
2	30	1-15	5	16	0.223	2.7	1:3	intravenously
3	27	1-20	5	19	0.278	2.5	1:2.9	intravenously
4	38	1-20	4	24	0.500	2.7	1:1,7	inhalational

Table 1.1: List of in-vivo subjects, their physical characteristics, used intra-abdominal pressures(IAP),mechanical ventilator settings and type of anesthetic used.

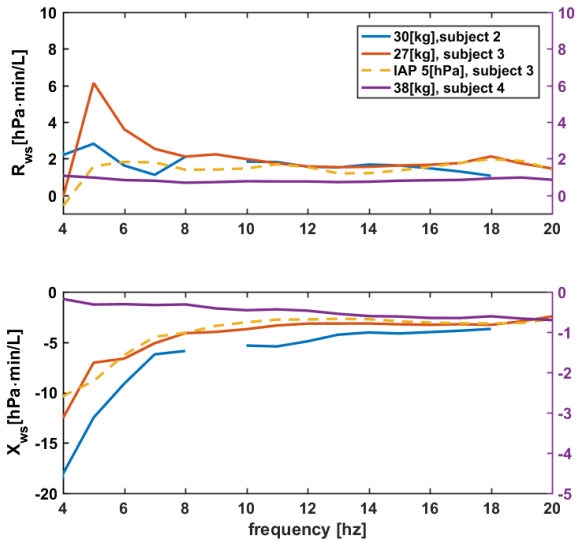

Figure 1.5: Results frequency sweeps at mean IAP 10 hPa for all subjects and an additional frequency sweep at mean IAP 5 hPa in subject 3, (–). Resistance(top graph) and reactance(bottom graph) are plotted against the forced pressure signal frequency used. The measurements in subject 4 are plotted on a different scale,(right side).

In subjects 2 and 3 initial pneumoperitoneum was obtained during the experiment. Subject 4, initial pneumoperitoneum was obtained previous to the experiment. The results are very different from results in subjects 2 and 3, a very low impedance was measured at all frequencies. The resistance component is only lower but in the same order of magnitude. The reactance component was close to zero and becomes more negative when the frequency is increased.

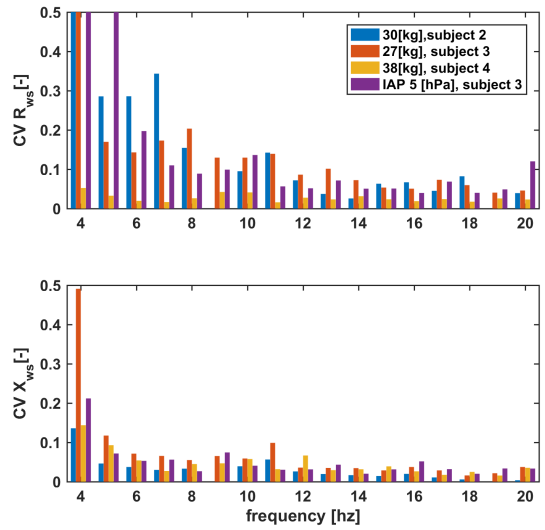

Figure 1.6: Coefficients of variation for the frequency sweep measurements presented in figure 1.5.

Figure 1.6 shows the calculated coefficients for the resistance and reactance. Overall the coefficient of variation for resistance is smaller than for reactance.

3.4. Pressure sweeps

The pressure sweep in subject 2 was done only up to 15 hPa. Full pressure sweeps were done in subject 3 and 4. In subjects 2 and 3 the resistance increases with mean IAP, the slope increased around 15 hPa. In subject 4 the resistance started at 0.21hPa · min/L] and increased up to 0.83 [hPa · min/L] at mean IAP 5 hPa. It remains constant when pressure is increased further.
In all subjects at mean IAP 1 hPa, the reactance is approximately zero. In all subjects the reactance decreased when mean IAP was increased. In subjects 2 and 3 the slope changes at 3 hPa, in subject 4 the change occurs at 6 hPa. The reactance in subject 4 was approximately 20 time smaller.

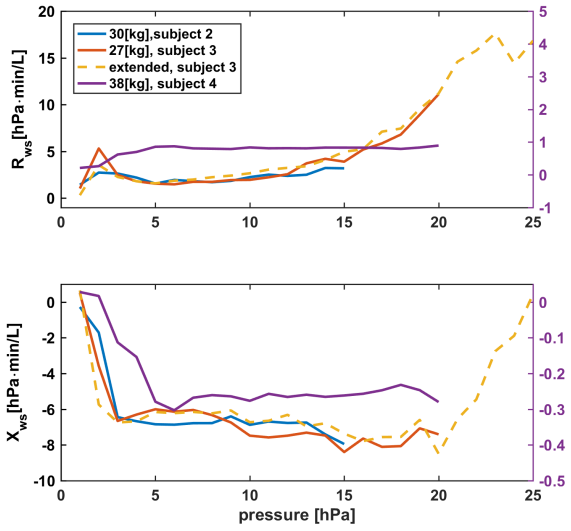

Figure 1.7: Results pressure sweeps using a forced pressure signal frequency of 6 Hz for all subjects. An extended pressure sweep was done in subject 3, (–). Resistance (top graph) and reactance(bottom graph) are plotted against the forced pressure signal frequency used. The measurements in subject 4 are plotted on a different scale, (right side).

An extended pressure sweep was done in subject 3 to identify the effect of exceeding the peak inspiratory pressure provided by the mechanical ventilator(19 hPa). The resistance appears to keep on increasing. A steep increase in reactance started at IAP 20 hPa.

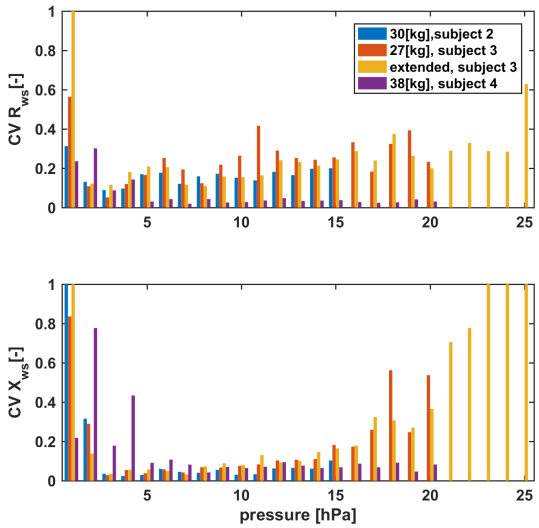

Figure 1.8: Coefficients of variation for the pressure sweep measurements presented in figure 1.7.

In both graphs can be seen that the coefficients are large at low mean IAP. In subjects 2 and 3, the coefficients of variation in for resistance are larger than for reactance. In subject 4 the coefficients are larger for reactance than resistance. The coefficients for reactance increases with mean IAP, in subject 3 the coefficient for reactance becomes larger than for resistance.

4. Discussion

The goal of this research was to determine if the forced oscillation technique could be used to monitor surgical working space compliance. Forced pressure signal have been applied in three in-vivo experiments.

4.1. Forced pressure signal and distortions

The endoscopic FOT setup used provided sufficient amplitude at the trocar. A less powerful forced pressure generator can be used when the resistance in the tubing and flow sensor are reduced. The forced pressure signal is not a perfect sine, the signal contains a lot of harmonic distortions. The forced pressure signal has sufficient amplitude compared to the noise level. At low frequencies the noise level is increased by the mechanical ventilator. Because all signals are bandpass filtered before analysis, both the harmonic distortions and ventilator noise did not affect the results.

It would be recommended to use a different type of forced pressure generator. The speaker has to operate outside the frequency range it was designed for. In the field of pulmonary FOT fan based systems have been introduced, [6, 7]. The mean IAP and forced pressure signal are provided by a single pressure source. Closed-loop controllers are used to create the required forced pressure signal, this enhances the signal quality. Using a closed-loop controlled power source and a flow sensor with a lower impedance would obviate the need for manual adjustment of the forced pressure amplitude and correction of mfrequency behaviour of the flow sensor.

4.2. Frequency behaviour

Unfortunately there was no information on the previously used pressures for creation of the pneumoperitoneum in subject 4. Overdistension already could have occurred, therefore no conclusions can be drawn on these results. The frequency sweeps performed in subjects 2 and 3 confirm the balloon model described in equation 1.3. It was expected that the resonance frequency would be within the measurement window. It appears to be at a higher frequency. At all frequencies used, the reactance was negative. This in combination with the model in equation 1.3 proves that the 6 Hz used in the pressure sweeps provides information on changes in surgical working space compliance.

4.3. Surgical working space compliance

The behaviour seen in pressure sweep results confirms the hypothesis that the forced oscillation technique can be used to monitor surgical working space compliance. In all subjects the behaviour is similar. At low mean IAP it is easy to increase the volume, a finding supported by measurements of a low resistance and impedance. The exact cause for the increase in resistance is unknown. The mechanical ventilator counteracting the volume increase of the surgical working space could be the cause. Calibration of the measurements took place in a reference impedance without mechanical ventilation. No increase of resistance was seen in this reference impedance.

The change in reactance in the extended pressure sweep can be explained by the mechanical ventilator pressure control mode. When the peak inspiratory pressure is exceeded a pressure release valve opens in the mechanical ventilator. The mechanical ventilator stops counteracting the increase in surgical working space and the reactance becomes zero. This also explains the large coefficient of variation, μ/σ. The standard deviation remains constant but the absolute mean decreases.

4.4. Statistics and safety

The scientific strength of the results presented is limited. The two main reasons low sample size and no direct comparison to the golden standard: volu-

metric CT-measurements. Yet the results of this research are strong enough to pursue further research on endoscopic FOT. From observations during the experiments this technique seems to be a safe way of monitoring surgical working space compliance. The forced pressure signal had no noticeable effect on the ventilation and hemodynamics of the subjects.

4.5. Future work

In this research endoscopic FOT has only been applied during laparoscopy, but the concept seems to be transferrable to thoracoscopy and other endoscopic interventions. The initial frequency band used for the frequency sweeps was based on Coermann et al. [1]. In the last decade the frequency band used in pulmonary FOT has been expanded. Both very high and very low frequencies are being used to identify different properties within the respiratory system. A similar approach could be used in endoscopic FOT. The structure of the lungs is very different from the laparoscopic working space. The lack of a bronchial tree simplifies parameter estimation in endoscopic FOT. On the other hand the surgical working space has other properties that require more complicated models. Other organs, with their own impedance properties, reside within the surgical working space. The working space is surrounded by the abdominal wall, other organs and the diaphragm, figure 1.9. Multiple frequency bands could be used to identify their contribution to the total impedance. In pulmonary FOT, both low and high frequency perturbations are combined to determine the visco-elastic properties of the lung tissue. The 6 Hz frequency currently appears to monitor changes in volume. Still volumetric CT-scans are needed to verify if this frequency monitors changes in volume. For the monitoring of surgical working space compliance this would be sufficient. Directly detecting changes in tissue mechanics due to overdistension would require a broader band of force pressure frequencies.

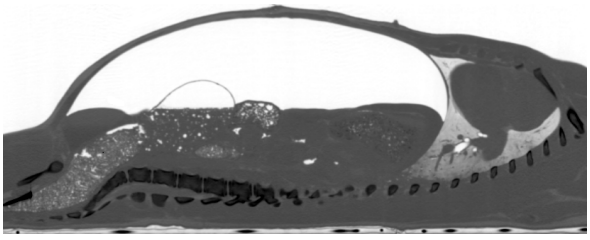

Figure 1.9: A single slice of a CT-scan of the laparoscopic surgical working space within a porcine mode. Source: Erasmus MC, inverted for clarity.

5. Conclusion

Thusfar the relation between intra abdominal pressure and the created volume has only been measured accurately using a CT-scans in animals [10]. This research shows the results of applying forced oscillations onto the surgical working space. It seems safe for the patient and provides information on changes in surgical working space compliance without prolonging the surgical procedure.
Although the scientific strength is limited, further research should be pursued. The scientific value can be strengthened by comparing this technique to the golden standard volumetric CT-measurements. Improvements can be made in terms signal generation and measuring the effects. Future work should focus on distinguishing the contribution of the surrounding tissues and clinical implementation of this technique. Investigation other frequency bands would not only provide new information on surgical working space compliance but it would also aid in understanding the interaction with mechanical ventilation.

Bibliography

[1] ROLF R Coermann, GH Ziegenruecker, AL Wittwer, and HE Von Gierke. The passive dynamic mechanical properties of the human thorax-abdomen system and of the whole body system. *Aerospace medicine*, 31(6):443–455, 1960.

[2] Raffaele L Dellacà, Alessandro Gobbi, Miriam Pastena, Antonio Pedotti, and Bartolomè Celli. Home monitoring of within-breath respiratory mechanics by a simple and automatic forced oscillation technique device. *Physiological measurement*, 31(4):N11, 2010.

[3] Arthur B DuBois, Alfred W Brody, David H Lewis, and B Franklin Burgess. Oscillation mechanics of lungs and chest in man. *Journal of Applied Physiology*, 8(6):587–594, 1956.

[4] David W Kaczka and Raffaele L Dellaca. Oscillation mechanics of the respiratory system: applications to lung disease. *Critical Reviews™ in Biomedical Engineering*, 39(4), 2011.

[5] David W Kaczka, Edward P Ingenito, and Kenneth R Lutchen. Technique to determine inspiratory impedance during mechanical ventilation: implications for flow limited patients. *Annals of biomedical engineering*, 27(3):340–355, 1999.

[6] Hannes Maes, Miroslav Zivanovic, Johan Schoukens, and Gerd Vandersteen. Estimating respiratory impedance at breathing frequencies using regularized least squares on forced oscillation technique measurements. *IEEE Transactions on Instrumentation and Measurement*, 2017.

[7] Oscar Olarte, Robin De Keyser, and Clara M Ionescu. Fan-based device for non-invasive measurement of respiratory impedance: Identification, calibration and analysis. *Biomedical Signal Processing and Control*, 30:127–133, 2016.

[8] E Oostveen, D MacLeod, H Lorino, R Farre, Z Hantos, K Desager, F Marchal, et al. The forced oscillation technique in clinical practice: methodology, recommendations and future developments. *European Respiratory Journal*, 22 (6):1026–1041, 2003.

[9] HJ Smith, P Reinhold, and MD Goldman. Forced oscillation technique and impulse oscillometry. *European Respiratory Monograph*, 31:72, 2005.

[10] John Vlot, René Wijnen, Robert Jan Stolker, and Klaas N Bax. Optimizing working space in laparoscopy: Ct measurement of the effect of prestretching of the abdominal wall in a porcine model. *Surgical endoscopy*, 28(3):841–846, 2014.

[11] John Vlot, Patricia A Specht, René MH Wijnen, Joost van Rosmalen, Egbert G Mik, and Klaas MA Bax. Optimizing working space in laparoscopy: Ct-measurement of the effect of neuromuscular blockade and its reversal in a porcine model. *Surgical endoscopy*, 29(8):2210–2216, 2015.

[12] DH Wallace, MG Serpell, JN Baxter, and PJ O'dwyer. Randomized trial of different insufflation pressures for laparoscopic cholecystectomy. *British journal of surgery*, 84(4):455–458, 1997.

A

Appendix: Experimental setup and mechanical drawings

1. Design EndoFOT setup

EndoFOT setup

Design report

Table of Contents

Problem Definition

This chapter is divided into three sections to give an introduction to the design problem. First, the scope of this design project will be described. A brief technical review of similar designs used for Forced Oscillation Technique setups is given in section Technical review. The design requirements are given in the section Design Requirements.

Problem Scope

The whole design problem starts with the idea that it might be possible to monitor surgical working space compliance by applying the Forced Oscillation Technique(FOT) endoscopically. To put this idea to the test an endoscopic FOT setup is needed. This setup should enable the user to apply oscillatory pressure perturbations and measure the effects in terms of pressure and flow.

Technical review

background

In minimal access surgery having a large surgical working space is beneficial. It is easier to operate and this shortens the procedure. Enlarging the surgical working space can be done by increasing the insufflation pressure. This increased pressure can have adverse effects. Additional carbon dioxide uptake into the blood stream. The pressure used for insufflation opposes the pressure created for ventilation. Usually, over-distention of the tissues surrounding the surgical working space usually is the first problem when increasing the insufflation pressure. Surgical working space compliance describes the relation between insufflation pressure and created surgical working space. Every patient has a different working space compliance, it is mainly affected by body size, weight, and age. In current practice, every patient is insufflated using a certain insufflation pressure, if more space is needed the pressure is increased further. Commonly surgeons are not aware of the fact that compliance can change due to over-distention and mechanical ventilator settings.

Multiple techniques are available to monitor surgical working space compliance, yet all of them are only applied for experimental purposes. Measuring pressure is simple compared to volumetric measurements. At this point, CT-volumes are considered the golden standard. Another method is the use of markers to detect over- distention. Both methods seem to be impracticable for continuous monitoring of a patient during surgery.

In mechanical ventilation, the forced oscillation technique only requires pressure and flow sensors. Both physical quantities are already monitored by the current generation of insufflation devices, but on a very low sample rate. Thereby, the high frequency Forced Oscillations could not be created by an insufflator. Mechanical ventilators are capable to measure pressure and flow at high sample frequencies. They can create the high perturbation frequency, but cannot be used to insufflate carbon dioxide into the surgical working space because of their bias flow. My first try was to adapt the mechanical ventilator in such a way that it could be used for insufflation purposes. Bypassing the controller, to use carbon dioxide instead of air, turned out to be impossible. Therefore, it was decided to build a setup specifically to test if the forced oscillation technique could be used to monitor the surgical working space compliance.

Prior art technology

The forced oscillation technique was first described by Dubous et al. in 1953. In this article two methods were proposed for measuring chest wall impedance. Voluntary breathing patients were used for his research and there was no need to apply a mean pressure to the airway opening of the patient. The forced pressure oscillations were provided by a piston mechanism. Forced pressure frequencies between 2 and 15 Hz were applied. Chest wall velocity, pressure and flow were recorded on paper using a cathode-ray oscillography.

A review of various techniques to acquire impedance data in both clinical and research settings was given by Kaczka et al. The review provides a theoretical background on instrumentation, signal processing and inverse modelling. Inverse modelling is used for diagnostic purposes. A setup used for detection of expiratory flow limitation is presented by Dellaca et al., figure 3.

A review by Oostveen et al. presented a set of guidelines for FOT in clinical practice. A peak-to-peak size of the composite signal of 1-3 hPa seems optimal. The coefficient of variation should be presented for every measurement to compare between patients. In the last decade, the band of forced pressure frequencies has been expanded. Low frequencies, 0.25–5 Hz, could be used to identify tissue properties and high frequencies, +/-100 Hz, can be used to identify airway obstructions. The response to low frequencies commonly requires a respiratory pause.

The need for compact devices, used for home monitoring, and the need to create low frequency forced oscillations has led to the use of in line-turbines. Figure 1 shows a setup using two turbines to create a forced pressure signal at the airway opening.

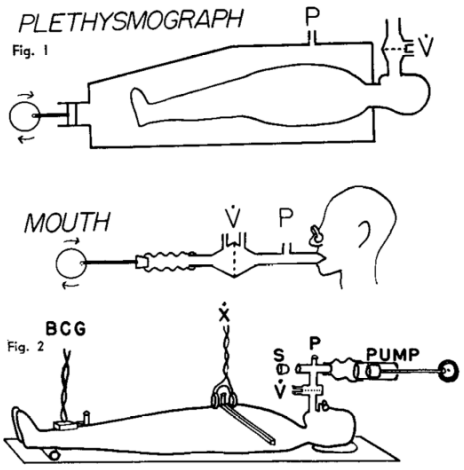

Figure 2: First Forced Oscillation Technique setup by Dubois et al, 1953

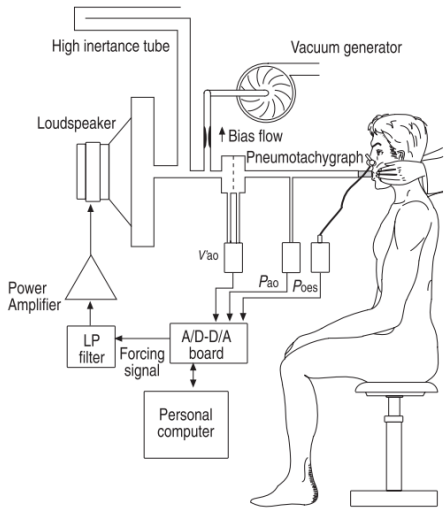

Figure 3: FOT setup used by Delaca et al. 2004.

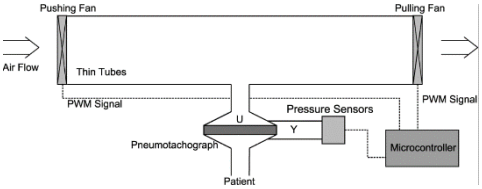

Figure 1: FOT setup using turbines Meas et al. 2017

Design Requirements

There are three key requirements when it comes to the EndoFOT setup. First, there is the ability to create a forced pressure oscillation signal. No signal no measurements. Secondly, there is the ability to measure the response in terms of pressure and flow. Thirdly, there is safety, both user and patient should be protected from harm. There are some additional requirements but these are not leading in terms of design.

Perturbation

The setup should be able to do sine sweeps at multiple pressure levels. The amplitude of these oscillations should be at least 2hPa peak-to-peak, measured at the trocar. The bandwidth of interest is 2-20hz, the setup should be able to create these signals. The mean pressure levels could range up to 40hPa the setup should be able to provide these pressures.

Measurements

The setup should be able to measure both flow and pressure. The maximum pressure provided by the insufflator is 40hPa. The insufflation pressure plus or minus the perturbation pressure should be measurable. The requirement was set 50hPa. For flow the range is based on mechanical ventilation, the requirement was set to 20 L/min. The sampling frequency should be high enough to measure the perturbation frequencies. The max frequency will be 20hz therefore the sampling frequency should be at least twice this value, 40hz.The pressure transducers are connected to the power grid. Because of the 50hz operating frequency this the sampling frequency of the data acquisition should be at least double this value, 100hz. Both measurements should be done close to the trocar. The frequency behaviour of the system should be flat up to 20hz.

Safety

The setup will be perturbing Endoscopically. Perturbing with a 2hPa peak-to-peak sinus is assumed to be safe. Other peak pressures, >50hPa, should be prevented. The amount of CO2 leakage should be kept to a minimum, less than 1 L/min. The device should also be electrically safe. The device should be safe to use for both the user/surgeon and the patient.

Other requirements

There are multiple other requirements. Firstly, the data obtained during experiments should be stored for later analysis. Secondly, some components are available within the Erasmus MC, the setup should be compatible with these components. Components can be replaced, this can only be done after consultation with the supervisors. The components available are: a Karl Storz Endoflator 40, with insufflation tubing, a NI DAQMX USB-6001, a Respironics flow sensor piece and an old trocar.

Design Description

Overview

The whole design can be best describe using the pneumatic-electric analogy. The pneumatic circuit can be drawn as an electric one, pressure equals voltage, flow equals current. Figure 4 shows this circuit, the Karl Storz Endoflator will be set parallel to a speaker. This way both AC and DC are created separately. A manifold should combine both signals and convey them through the insufflator tube to the trocar. Near the trocar both flow and pressure are measured. The flow probe by Respironics will behave like a resistance, R2. The rest of the system represents the surgical working space behaviour. All pressures are relative to the pressure in the atmosphere, therefore this can be considered a ground.

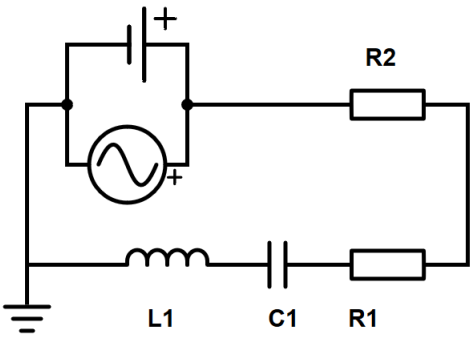

Figure 4: EndoFOT electrical circuit analogy. The DC signal is created by the Karl Storz Endoflator and the AC signal is created by the Pioneer speaker. These two devices are described by two voltage sources parallel. Resistance within the flow sensor is represented by R2. The impedance behaviour by the surgical working space and trocar is given by the inductor, capacitance and resistance. All pressures are measured compared to the room pressure, this is represented by the ground.

Figure 5 shows the schematics of the rest of the design. Pressure and flow are measured. Before analog-to-digital conversion, by the DAQMX, the electrical signals have to be filtered. A computer will be used for analysis to determine the resistance and reactance. The speaker is actuated by a power amplifier, the signal for this amplifier is created on a computer.

Detailed Description

It was mentioned before, some of the components were already available. The Karl Storz Endoflator and Respironics flow piece will be used. The DAQMX-USB6001 had to be replaced with the DAQMX-USB6211. The old trocar will be customized to be able to connect to the flow piece.

Loudspeaker and power amplifier

The speaker is the key component when it comes to perturbation. A large subwoofer should be used. For pulmonary FOT, 200W subwoofers are used. In this design the TS-W261D4 Pioneer was chosen. It has a nominal output power of 350W and could be set to have 8Ω electrical impedance. A higher nominal power was chosen because CO2 has a larger density than air, 1.977 kg/m3 vs 1.184 kg/m3. This would result in a higher resistance of the flow sensor and in the tubing. Besides the volume can always be lowered if the speaker appears to be overpowered. A normal audio amplifier will be used, the American Audio VLP1500 was chosen for this purpose. It has a switch to bypass the built-in high-pass filter, to prevent DC signals. A mono-sound output setting is available, then it can provide up to 1500W power

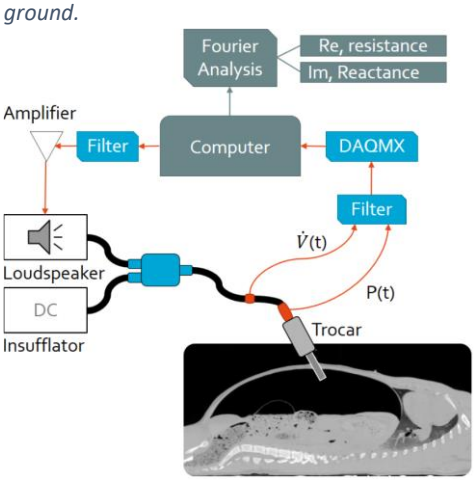

Figure 5: Experimental set-up for Endoscopic input impedance measurements. The insufflation pressure and flow are measured close to the trocar.

Container and manifold

The carbon dioxide gas should stay within the system. A container surrounding the speaker was designed. For proper functioning of the speaker, the pressure in front and behind the speaker should be equal. The container will also be used to convey the gas into a 19mm hose. The diameter of this

hose is relatively large, this is done to keep the impedance as low as possible. This way the created pressure will actually reach the manifold.

Combining the signals will take place in the manifold. In the case of a system malfunction, the manifold is the place where the peak pressure can be measured and stopped. A pressure release valve will be connected, this way pressures higher than 50hPa will be prevented. The connector from the Karl Storz

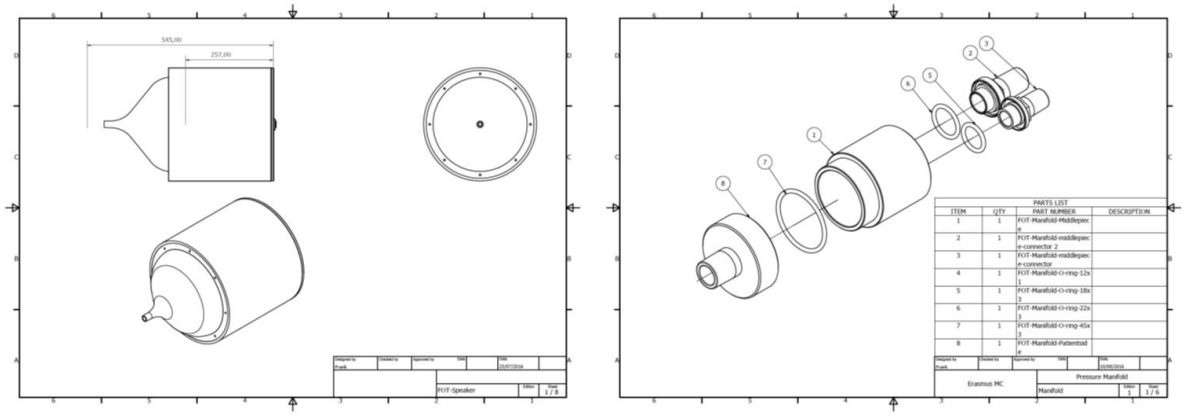

Figure 6: Mechanical assembly drawings for the container and manifold, full drawings are included in the appendix.

Endoflator to the manifold and the connector from the manifold to the trocar should be manufactured according to ISO5356-1-2004. The mechanical assembly drawings are shown in Figure 6.

Sensors and analog filter

Two pressure transducers will be used to measure the flow in the Respironics flow piece. A third pressure transducer is needed for actual pressure measurements. In this design, there will be four pressure transducers. In case one of the pressure transducers fails during measurements the fourth one can be used as a replacement. By having four transducers, two Respironics flow pieces could be connected.

The HCS160MD pressure transducers were chosen. They have a response time of 1ms and measure up to 160hPa. A 5V power source and an analog low pass filter are required for these sensors. The filter is designed to have a 100hz cutoff frequency. The DAQMX is used to convert the analog signal to digital signals. Within Labview digital filters are used to suppress high-frequency disturbances.

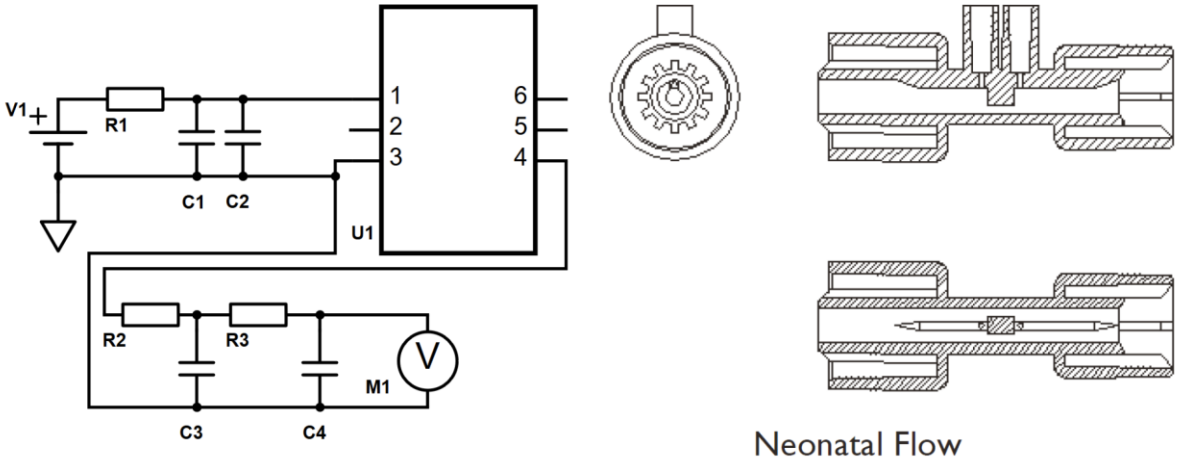

Figure 7: Overview low-pass filter for transducer and Respironics flow piece. Left side, electrical components: V1 DC-voltage source 5V; R1 4.7Ω; C1 0.1µf; C2 10µf; U1 Transducer, 1 and 3 power, 4 signal; C3 10µf; C4 1µf; R2 100 Ω f; R3 1000Ω; M1 Voltage measurement DAQMX. Right side, Respironics neonatal flow piece, source: Respironics white-paper.

Trocar

The old trocar should be modified, the pressure sensor and flow piece should be connected to the trocar. This can be done using regular connector pieces used for mechanical ventilation.

Use

The whole EndoFOT setup can be controlled from a computer. The computer is connected to the amplifier by a 3.5mm jack. The DAQMX transfers data through a usb-cable. The Karl Storz Endoflator is controlled through a usb to serial cable. A graphic user interface was made in Labview, the program and interface are described in the appendix.

The trocar should be put in place by a surgeon. After this the EndoFOT setup can be connected to the trocar. The computer will be used to control the forced oscillation frequency and pressure supplied by the Karl Storz Endoflator. The volume can either be adjusted on the amplifier or by the computer.

Evaluation

Overview

The EndoFOT setup will only be used for experiments. Modelling every component would be too cumbersome for this approach. A prototype was built the manufacturing process is described in the prototype section. For flow and impedance calibration the setup was connected to a gas tank. This way the frequency and pressure response of the system could be analysed.

Prototype

The whole EndoFOT setup was build and put onto a trolley for easy transportation, Figure 8. The power amplifier and insufflator were put on the bottom shelf. On top there is the Karl Storz Endoflator and a module for the the usb communication. The speaker was mounted on the top shelf. The drawings for the manifold were used for manufacturing. The 19mm tubing from the insufflator and speaker conveys the gas to the manifold. The blue components are the casings for the analog filters and pressure transducers. The white box is the DAQMX used for analog to digital conversion. An additional filter was placed after at the insufflator outlet for hygienic purposes.

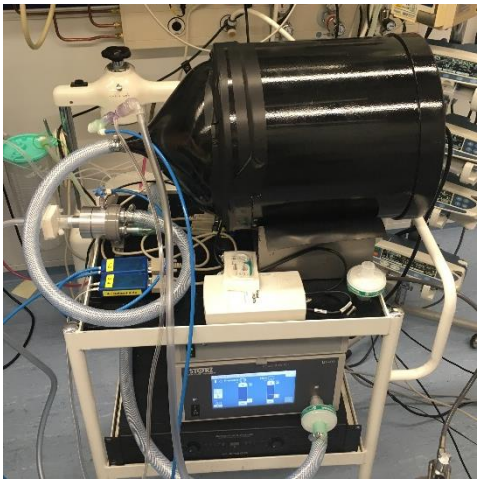

Figure 8: The EndoFOT setup on a trolley

Manufacturing

The speaker has been bought and the amplifier was borrowed. First the speaker was built into the container. The conical piece was vacuum-formed using a 3d-printed mold. The components for the manifold were manufactured and assembled. The safety valve, model AV319 was bought from Wittgas. This valve and the Luer-lock connector were screwed onto the manifold. The trocar was modified. The sensors and analog filter were soldered and put into their casing.

Figure 9: manufacturing of the EndoFOT setup. The speaker within the CO2 container; the cone piece and mold; Sensors for data acquisition with manifold components. The customized trocar.

Testing

Perturbation

The pressure signal created is not a perfect sine. A lot of distortion is present, this is mainly due to the very low frequencies used. A speaker cone is designed to actually move at higher speeds, without reaching the maximum displacement. What can be seen in the graph is the high-pressure peaks from the cone moving through the equilibrium point. In between these peaks, the cone reaches its maximum displacement. This causes harmonic distortions of the signal. The volume control is done by hand. Estimating the amplitude of the actual perturbation is difficult. In this 6hz sample it can be seen that the actual perturbation amplitude is 1hPa instead of the intended 2hPa peak-to-peak.

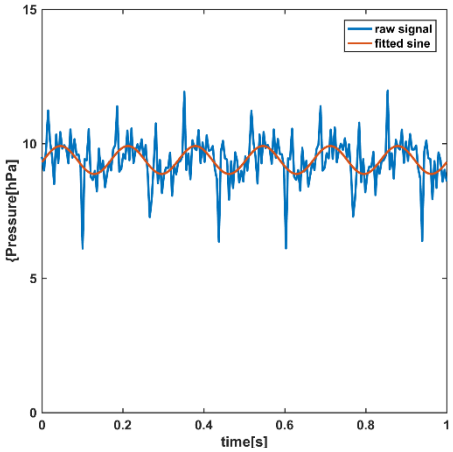

Figure 10: The perturbation pressure near the trocar at 6hz.

This perturbation is not due to the lack of power of the speaker. The perturbation pressure measured in the manifold is 6hPa peak-to-peak, Figure 11. A large pressure drop is caused by the tubing between the manifold and the trocar. This can be either the insufflation tube or the Respironics flow piece. The pressure is also measured just before this piece. From Figure 12 it can be seen that the pressure drop in the insufflation tube is negligible. The pressure drop is mainly due to the resistance within the Respironics flow piece.

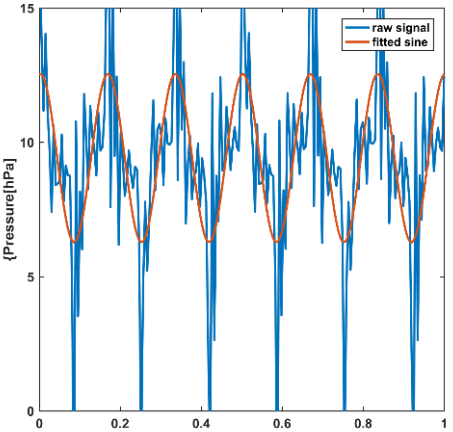

Figure 11: The perturbation pressure in the manifold at 6hz.

The Karl Storz Endoflator

From figure 6,7 and 8 it can also be seen that the pressure provided by the insufflator is too low. In the measurements shown in the figure the mean pressure was set to 10hPa. In table 1 the target pressure and measured pressure are presented. At higher mean pressure, the deviation is more than 1hPa. No measurements were taken near the outlet of the insufflator.

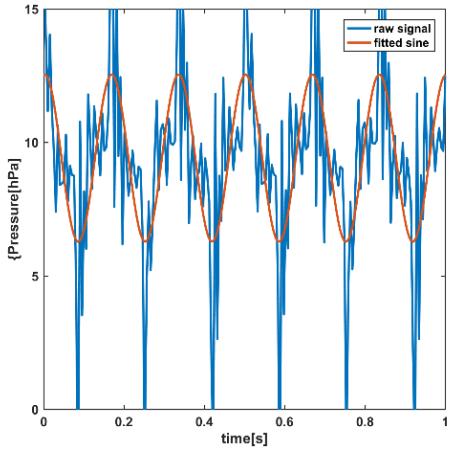

Figure 12: The perturbation pressure before the Respironics flow piece at 6hz.

Table 1: Comparing target pressure and measured mean pressure

Target[hPa]	1	2	3	4	5	6	7	8	9	10
Measured[hPa]	1.15	1.69	2.64	3.69	4.46	5.56	6.51	7.37	8.40	9.35
Target[hPa]	11	12	13	14	15	16	17	18	19	20
Measured[hPa]	10.26	11.30	12.16	13.10	14.09	15.21	16.14	17.09	17.99	18.83

Measuring

The flow measurements could be verified by connecting the whole setup to a CO2 gas tank instead of a trocar. An old gas tank was modified and its volume was measured. Carbon dioxide is compressible. From calculations, the change in volume can be determined and this change should correspond to the flow measured by the EndoFOT setup.

Figure 13: Connection piece reference gas tank

Safety

The whole setup was used in animal experiments. Before this it was verified that the pressure release valve would actually open when the pressure would exceed 50hPa. This was indeed the case. From observations during the experiments, it can be stated that the perturbations are harmless when compared to the effects of the DC pressure. Assessment.

Calibration

The sensors used in this setup should be calibrated, their measurements should not be affected by the mean pressure or frequency used for perturbation. The Respironics flow piece was designed for air, not for CO2.

Pressure

The transducers behave linearly within their operating range. Three points were used to calibrate all four sensors. The calibration curves are plotted in Figure 15. The calibration coefficients used of Labview are shown in

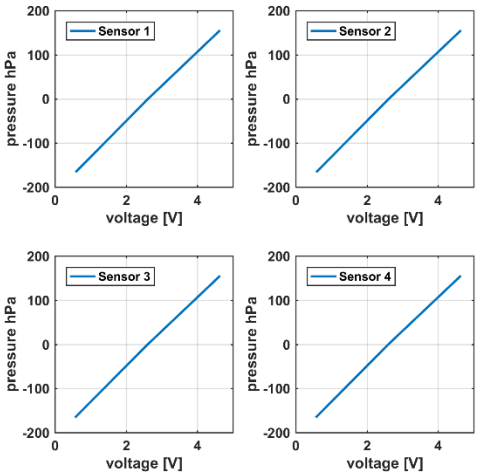

Figure 15: Pressure sensor calibration curves.

Sensor no.	1	2	3	4
dp/dV [hPa/V]	79.248	79.108	78.824	78.854x
Offset[hPa]	210.17	209.89	208.6	208.56

Table 2.

Figure 14: Numerical values calibration.

Table 2: Labview coefficients.

Sensor no.	1	2	3	4
dp/dV [hPa/V]	79.248	79.108	78.824	78.854x
Offset[hPa]	210.17	209.89	208.6	208.56

Flow

The pressure-behaviour was used to determine the calibration curve. Respironics provided a white-paper on the flow behaviour within a fixed orifice flow sensor.

$$F\left[\frac{L}{min}\right] = \frac{T_s}{T_m}\frac{p_m}{p_s} K \sqrt{\Delta p}$$

The flow is a product of the temperature ratio, $\frac{T_s}{T_m}$, and pressure ratio, $\frac{p_m}{p_s}$. The small m stands for the measured value near the sensor. The s stands for the temperature at the standard condition, the calibration temperature and pressure used. The factor K is geometric coefficient and should be

determined. The pressure drop over the flow sensor is proportional to the square of the flow, hence the square root. The pressure should be inserted in cmH2O, which equals hPa.

The coefficient for K should be determined because a different type of gas is used instead of air. This was done by connecting the flow probe to a flow calibration system that can be used for carbon dioxide. The result of these measurements is shown in Figure 14. Matlab was used to determine the K-coefficient using a function fit script. The code used is provided in the appendix. The value of K was determined to be 6.712.

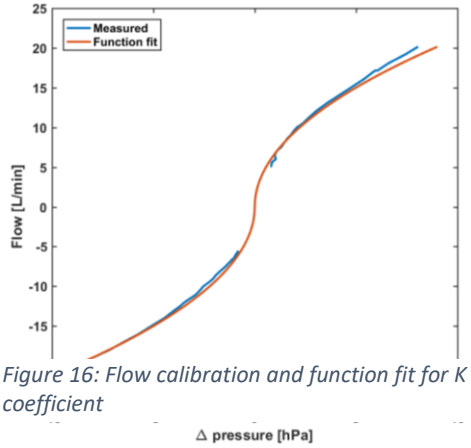

Figure 16: Flow calibration and function fit for K coefficient

Impedance

The calculated impedance has to be corrected for the frequency and pressure behaviour present in the EndoFOT setup. This was done by using a reference impedance the gas bottle from figure 10. The volume of this gas bottle is 3.573 liters.

The volume that passes through the flow sensor can be calculated. The change in pressure, compresses the gas and an additional volume will flow through the sensor into the bottle. This volume can be calculated based on the change in pressure and compressibility of the gas. The pressure close to the entrance of the gas bottle is used for these calculations. The absolute pressures should be used in this equation. The ratio between the minimal pressure and maximum pressure in one stroke should be taken. The compressibility factor gamma is 0.993 for carbon dioxide.

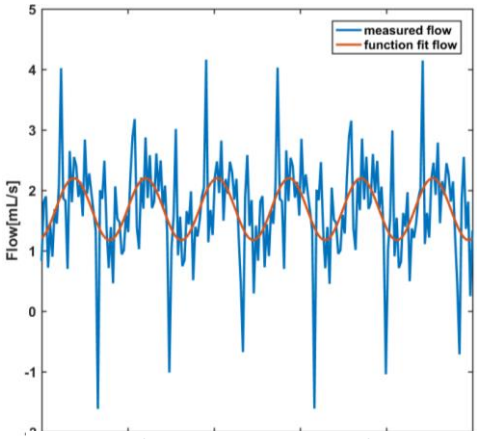

Figure 17: Flow measurements at the entrance of the gas bottle and function fit of sine flow.

$$\Delta V_{calc} = V_{ref} - \frac{p_{min}}{p_{max}} V_{ref}^{\gamma}$$

The average volume can also be determined by integration of the flow pattern. The sine function fitted onto the flow signal is used to determine the peak-to-peak flow amplitude, A. This amplitude should be multiplied by pi and divided by twice the frequency used. This is the analytic solution for integration of half a sine.

$$\Delta V_{meas} \frac{\pi A}{2f}$$

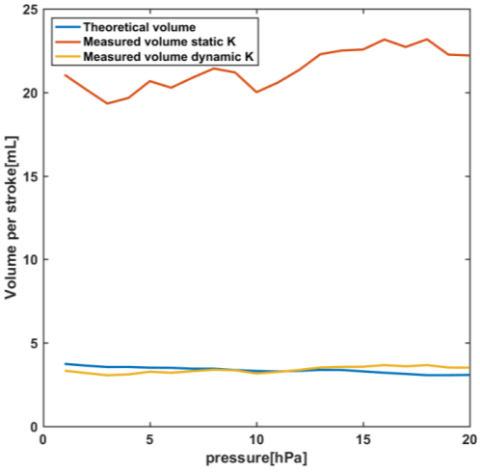

Figure 18: Estimated volume per stroke versus mean pressure.

Figure 14 shows the results of these volume estimated volumes per stroke. The measured volume overestimates the actual volume per stroke. If this remains uncorrected, the impedance will be overestimated. The K coefficient can be recalculated to correct this. This new dynamic K, 1.0622, will be used to estimate the flow. The flow is now corrected for the dynamic behaviour at 6 hz.

The frequency behaviour of the Respironics flow sensor should also be corrected. This was done by looking at a frequency sweep in the same gas bottle using the dynamic K. The same equations can be

used to determine the difference in measured and calculated volume. When using the new dynamic K, at high frequencies the volume is underestimated due to turbulence in the flow piece. The ratio between the calculated and measured for every frequency to compensate for the flow sensor impedance. The square root of this ratio should be taken to respect the relation between pressure drop and flow described in the whitepaper by Respironics. These are specific per frequency, table 3 shows these values.

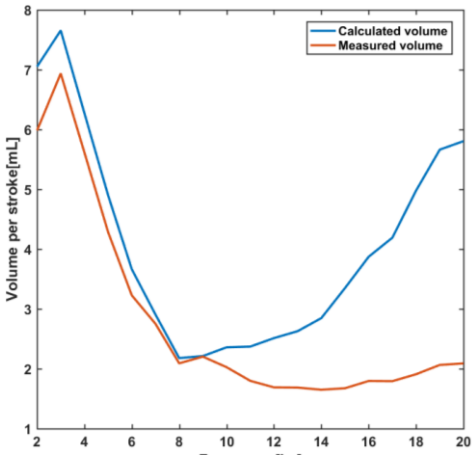

Figure 19: Result frequency sweep in gas bottle.

Frequency	**2**	**3**	**4**	**5**	**6**	**7**	**8**	**9**	**10**
K	1.0855	1.0506	1.0569	1.0694	1.0655	1.0278	1.0207	1.0022	1.0788
11	**12**	**13**	**14**	**15**	**16**	**17**	**18**	**19**	**20**
1.1481	1.2195	1.2487	1.3136	1.4142	1.4682	1.5290	1.6148	1.6562	1.6665

Table 3: Frequency dependent K's.

Recommendations

The whole setup meets the requirements for use in experiments. But there is still room for improvements. The system is able to produce sufficient amplitude for the forced oscillations. The signal is not a perfect sine, this causes harmonic distortions. Less filtering would be required if the signal would have fewer distortions. These distortions occur due to the mechanical behaviour of the speaker. Speakers are designed to create higher frequencies in the audible spectrum. The low frequencies used in this setup causes the coil to reach the limits of its suspension.

The Karl Storz Endoflator was used to provide the mean pressure. The discrepancy between the target pressure and actual pressure is probably caused by the controller used in this device. Peak pressures are prevented by the controller. The peaks, originating from the forced pressure oscillations, cause the controller to take action and lower the pressure output.

The first recommendation would be to integrate the generation of the mean pressure and forced oscillation pressure. An alternative for pressure generation could be a turbine in combination with a closed-loop controller. This would enhance the forced pressure signal quality because turbines are not limited by their suspension. The closed-loop controller could also be used to guarantee that the mean target pressure is reached.

The pressure measurements at the manifold and trocar don't leave a lot of room for improvement. The pressure transducers used for measuring flow in the Respironics flow sensor can be replaced by a single pressure transducer with a lower pressure range. From the calibration curves obtained the pressure drop over the sensor has a maximum of 10 [hPa]. Replacing this transducer will increase the resolution of the pressure drop.

It would be recommended to replace the Respironics flow sensor. It has been shown that the impedance of this flow sensor is frequency dependent. In other words, it has a certain flow body. Due to this, the measurements should be corrected for this behaviour. A flow sensor with a constant impedance behaviour in the frequency range would simplify analysis of the data. A smaller flow body would also require a smaller amplitude to be created by the speaker or turbine.

References

Dellaca, R. L., Santus, P., Aliverti, A., Stevenson, N., Centanni, S., Macklem, P. T., ... & Calverley, P. M. A. (2004). Detection of expiratory flow limitation in COPD using the forced oscillation technique. *European Respiratory Journal*, *23*(2), 232-240.

DuBois, A. B., Brody, A. W., Lewis, D. H., & Burgess, B. F. (1956). Oscillation mechanics of lungs and chest in man. *Journal of Applied Physiology*, *8*(6), 587-594.

Maes, H., Zivanovic, M., Schoukens, J., & Vandersteen, G. (2017). Estimating Respiratory Impedance at Breathing Frequencies Using Regularized Least Squares on Forced Oscillation Technique Measurements. *IEEE Transactions on Instrumentation and Measurement*.

Oostveen, E., MacLeod, D., Lorino, H., Farre, R., Hantos, Z., Desager, K., & Marchal, F. (2003). The forced oscillation technique in clinical practice: methodology, recommendations and future developments. *European Respiratory Journal*, *22*(6), 1026-1041.

Respironics (2011). Flow measurement with Respironics flow sensors. *White paper*.

2. Drawings manifold

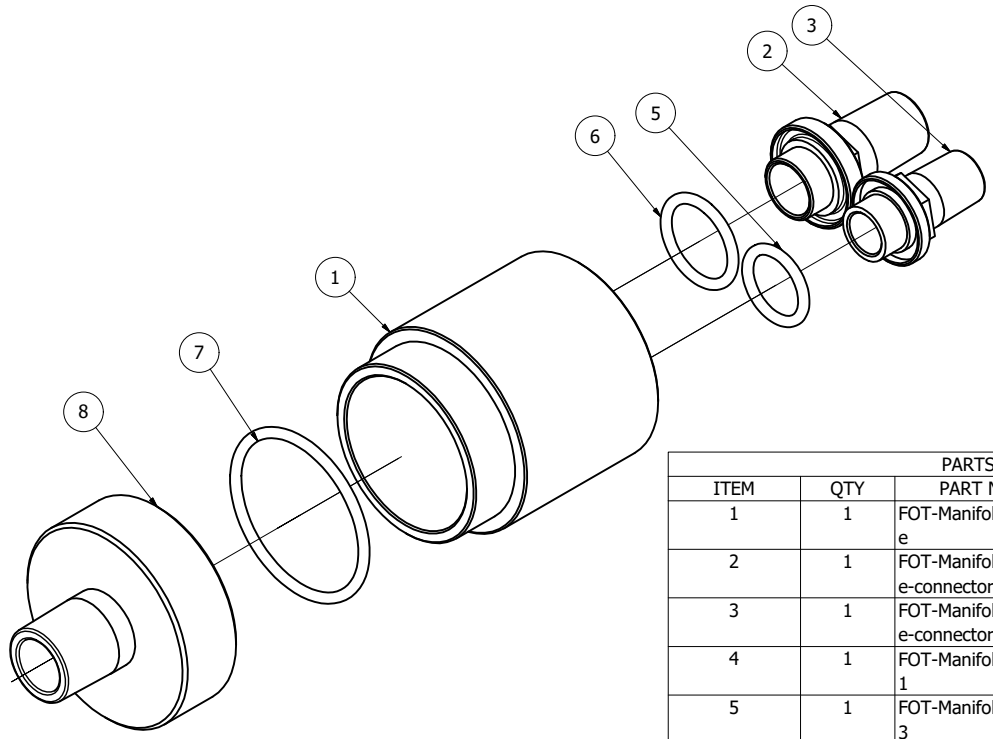

PARTS LIST			
ITEM	QTY	PART NUMBER	DESCRIPTION
1	1	FOT-Manifold-Middlepiece	
2	1	FOT-Manifold-middlepiece-connector 2	
3	1	FOT-Manifold-middlepiece-connector	
4	1	FOT-Manifold-O-ring-12x1	
5	1	FOT-Manifold-O-ring-18x3	
6	1	FOT-Manifold-O-ring-22x3	
7	1	FOT-Manifold-O-ring-45x3	
8	1	FOT-Manifold-Patientside	

Designed by	Checked by	Approved by	Date	Date
Frank				10/08/2016

Erasmus MC	Pressure Manifold		
	Manifold	Edition 1	Sheet 1 / 6

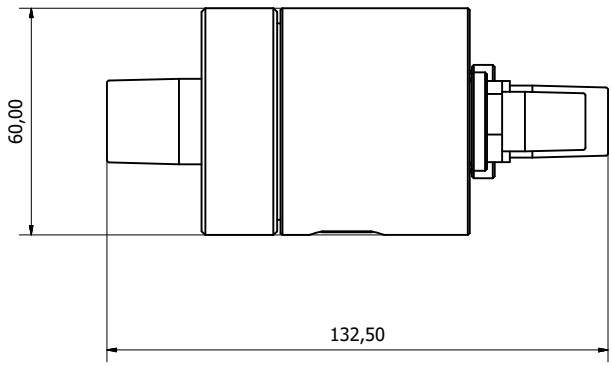

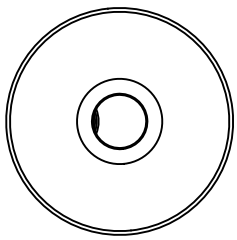

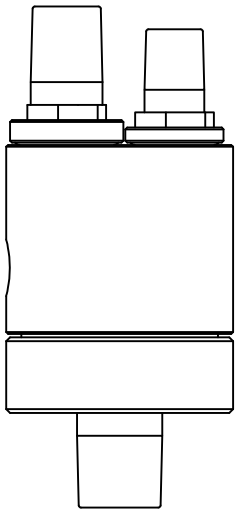

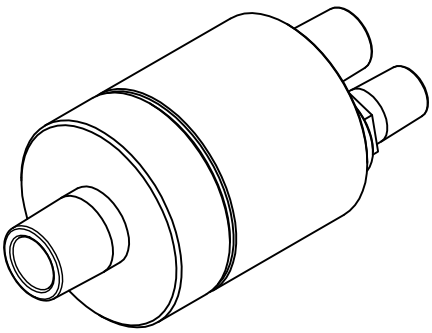

Designed by	Checked by	Approved by	Date		Date	
Frank					10/08/2016	

Erasmus MC	Pressure Manifold		
	Manifold	Edition 1	Sheet 2 / 6

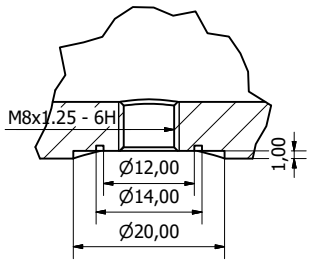

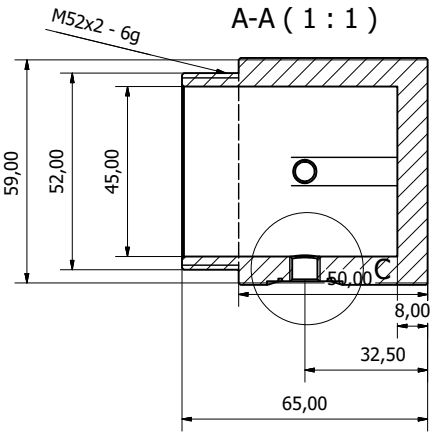

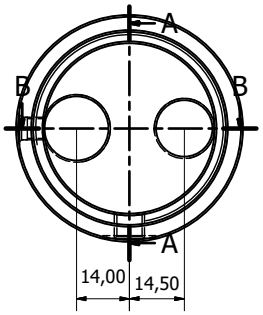

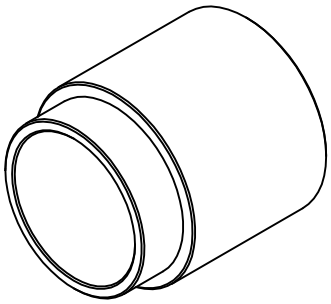

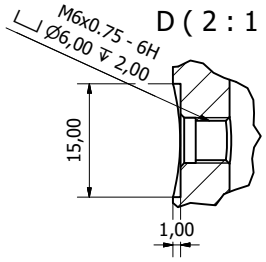

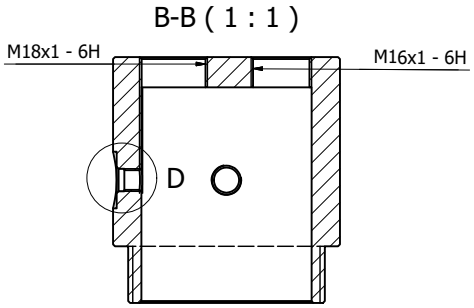

Designed by	Checked by	Approved by	Date		Date	
Frank					10/08/2016	

Erasmus MC	Pressure Manifold		
	Manifold	Edition 1	Sheet 3 / 6

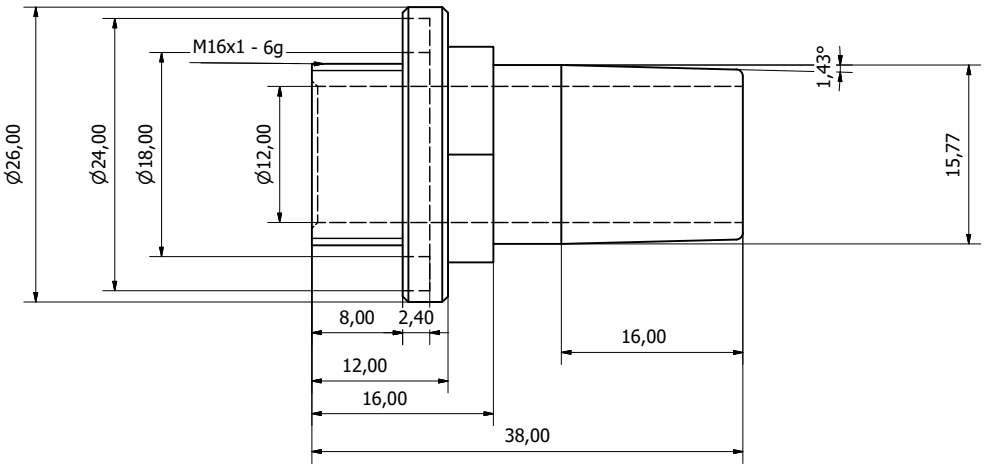

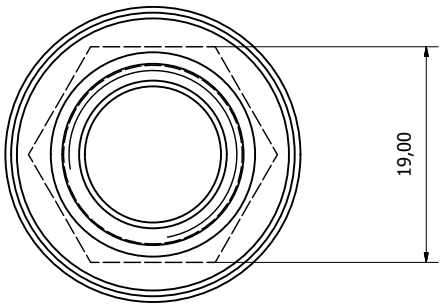

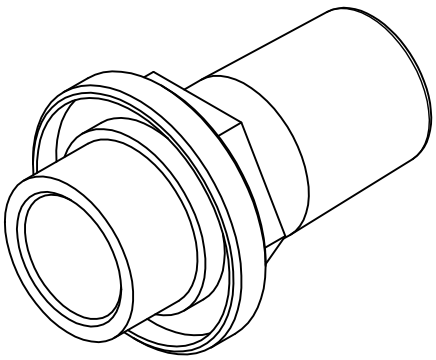

Designed by	Checked by	Approved by	Date		Date	
Frank					10/08/2016	

Erasmus MC	Pressure Manifold		
	Manifold	Edition 1	Sheet 4 / 6

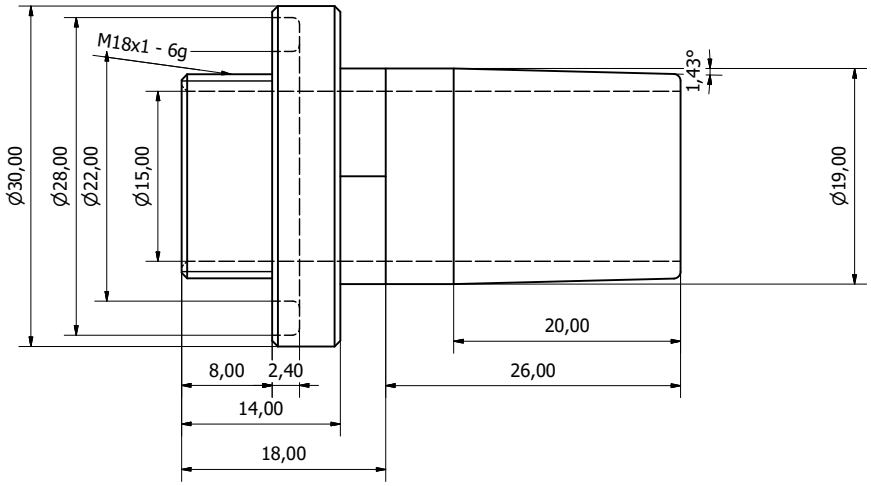

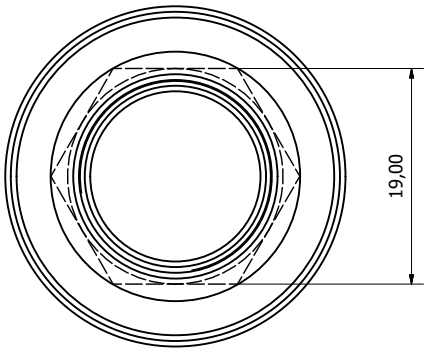

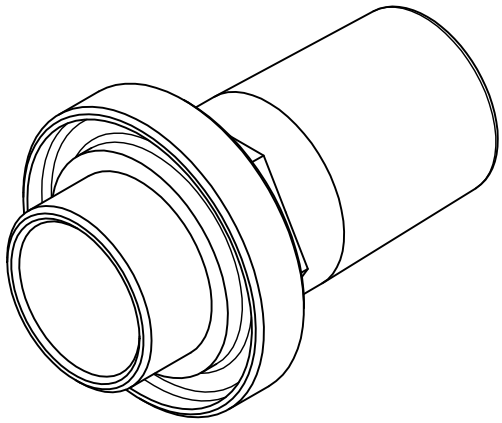

Designed by	Checked by	Approved by	Date		Date	
Frank					10/08/2016	

Erasmus MC	Pressure Manifold		
	Manifold	Edition 1	Sheet 5 / 6

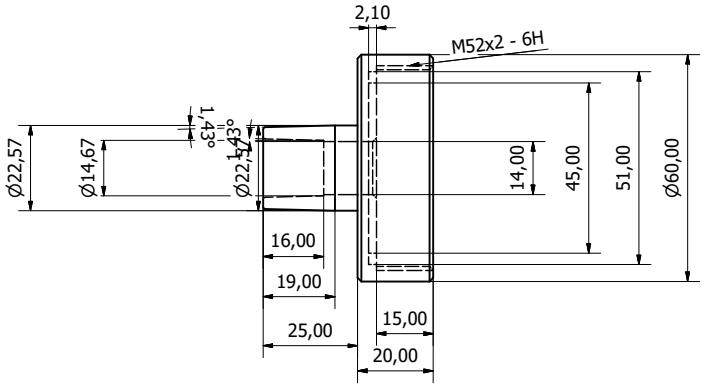

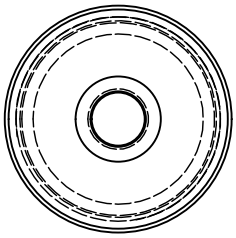

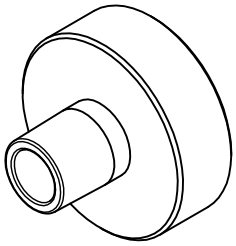

Designed by	Checked by	Approved by	Date		Date	
Frank					10/08/2016	

Erasmus MC	Pressure Manifold		
	Manifold	Edition 1	Sheet 6 / 6

3. Container and conical piece

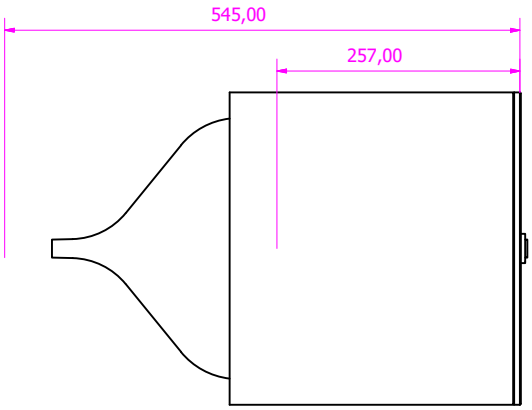

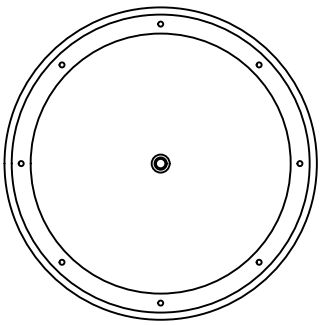

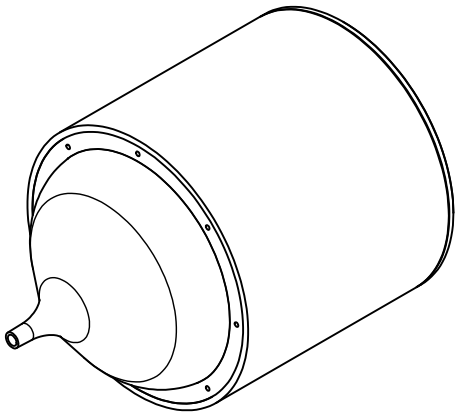

Designed by	Checked by	Approved by	Date		Date	
Frank					25/07/2016	

FOT-Speaker	Edition	Sheet 1 / 8	

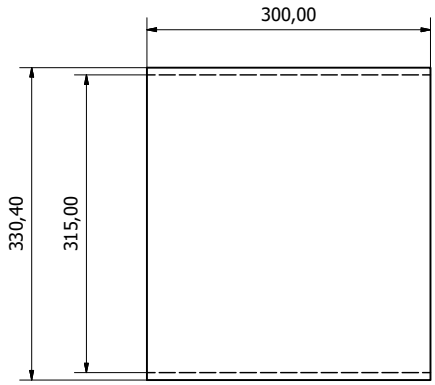

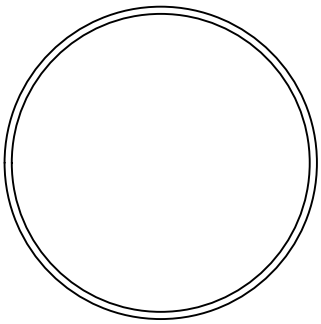

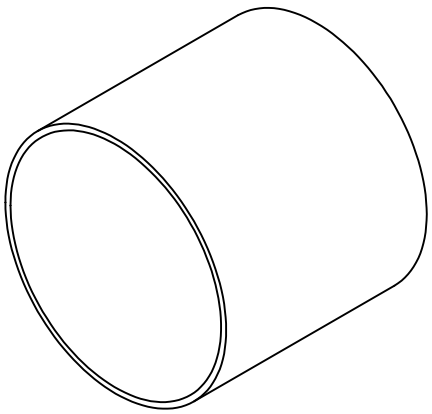

Designed by	Checked by	Approved by	Date		Date	
Frank					25/07/2016	

FOT-Speaker	Edition	Sheet 2 / 8

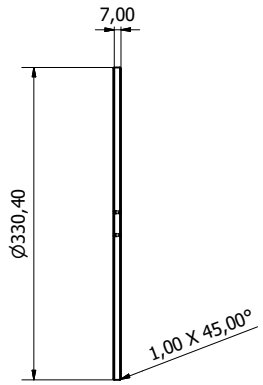

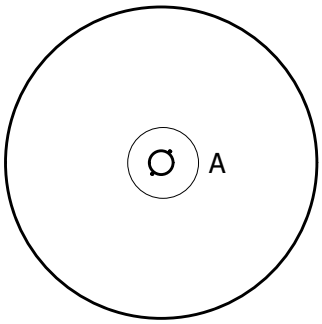

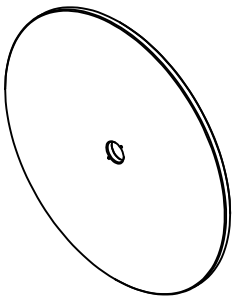

A (1 : 2)

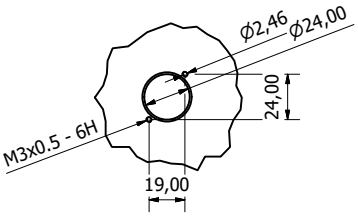

Designed by	Checked by	Approved by	Date		Date	
Frank					25/07/2016	

		Edition	Sheet
	FOT-Speaker		3 / 8

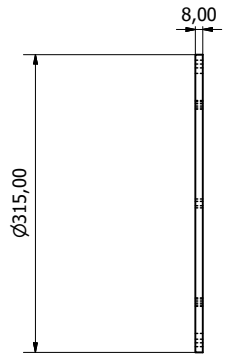

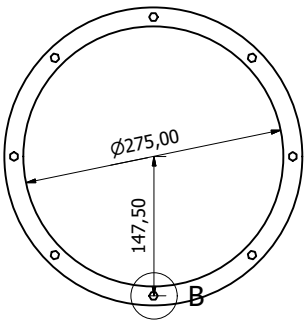

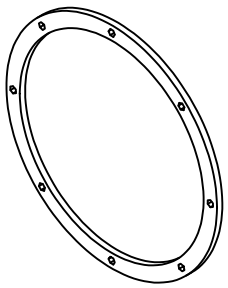

B (1 : 2)

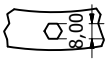

Designed by	Checked by	Approved by	Date		Date	
Frank					25/07/2016	

FOT-Speaker	Edition	Sheet 4 / 8	

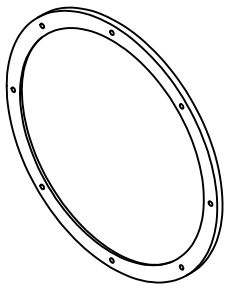

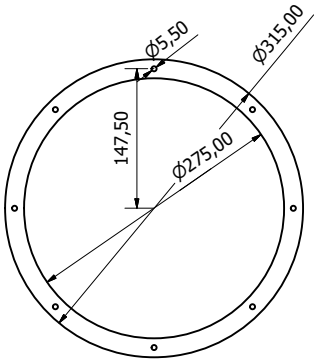

Designed by	Checked by	Approved by	Date		Date	
Frank					25/07/2016	

FOT-Speaker	Edition	Sheet 5 / 8	

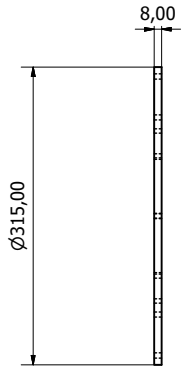

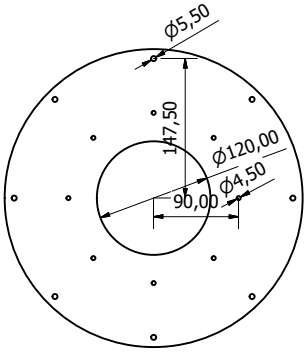

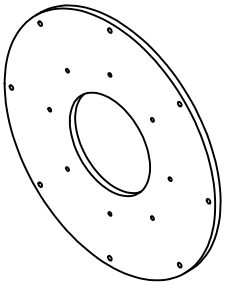

Designed by	Checked by	Approved by	Date		Date	
Frank					25/07/2016	

FOT-Speaker	Edition	Sheet 6 / 8	

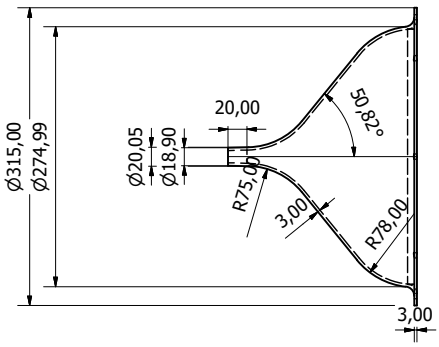

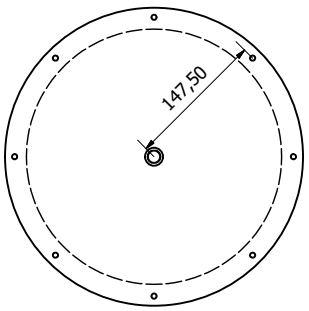

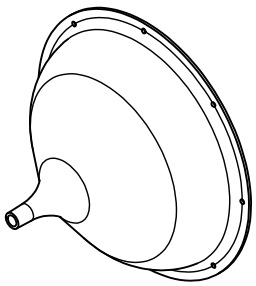

Designed by	Checked by	Approved by	Date		Date	
Frank					25/07/2016	

FOT-Speaker	Edition	Sheet 7 / 8	

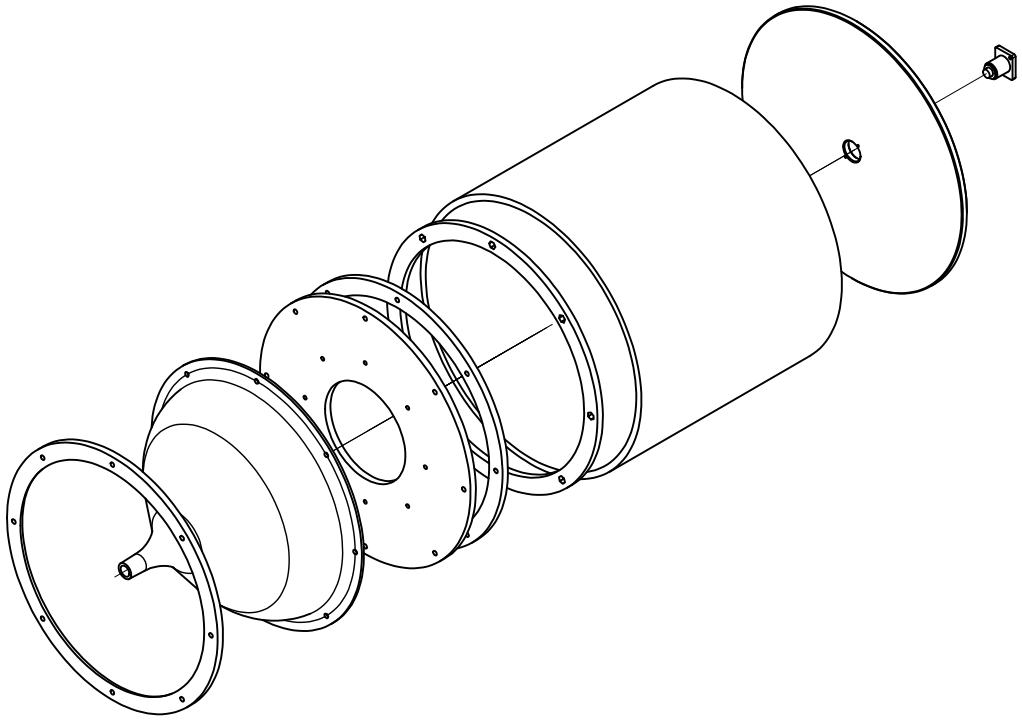

Designed by	Checked by	Approved by	Date		Date	
Frank					25/07/2016	

FOT-Speaker		Edition	Sheet 8 / 8

B

Appendix: Matlab code

1. Code to calculate K-coefficient for Respironics flow sensor

```
%% Flow calibration
close all; clear all; clc

load('C:\Users\Frank\Desktop\M sorted Data - Rewrite\Matlab Data files\M0S_FC.mat')
% Respironics whitepaper states: F = (Ts/Tm) * (pm/ps) * K * sqrt(delta p)
% In this case (Ts/Tm)= 1 = (pm/ps)
 dP_fit = linspace(-9,9,1001); % pressure range

dP(26)=nan;
 %% Function fit for K
G = 1; % Guess for K
Flowfunc  = @(G,K) G .* sign(dP).* sqrt(abs(dP));
K_fit = nlinfit(dP, F, Flowfunc , G);
F_fit = K_fit.*sign(dP_fit).* sqrt(abs(dP_fit));
figure(1)
plot(dP,F,dP_fit,F_fit,'LineWidth',2)
    legend('Measured','Function fit','Location','northwest')
    ylabel('Flow [L/min]')
    xlabel('\Delta pressure [hPa]')
set(gca,'FontName','Arial','FontSize',12,'FontWeight','Bold','LineWidth',1)
```

2. Code to calculate correction factors for frequency-sweeps impedance

```
%% Time graphs
clear all; close all; clc
load('C:\Users\Frank\Desktop\M sorted Data - Rewrite\Matlab Data files\M0S_SS_IAP10.mat')
A(1:6000,:) = R;
A = cat(3,A); % this 3 stands for 3rd dimension
clear R
fp = linspace(2,20,19);
IAP= 10*ones(k_max,1);

fs = 200;
Vref = 3.573/1000; % Inhoud ref impedance in mL

DC=zeros(k_max,2);
Amp=zeros(k_max,2);
measvol=zeros(k_max,1);
expvol=zeros(k_max,1);
K=zeros(k_max,1);
for j = 1:k_max
p_index     = ((j-1)*n_c)+3; % 3rd column in excel is pressure at the trocar

p2    = A(:,p_index);
p3    = A(:,p_index+1);
p4    = A(:,p_index+2);
% mean(K) = 1.0622 used for initial K
flow  = 1000./60.*(293.15./303.15).*((p3+1013.25)./1013.25)...
        .*1.0622.*sign(p3-p4).*sqrt(abs(p3-p4)); % Whitepaper Respironics
Data = [p2 flow];

for i = 1:2;
N = length(Data(:,i)); %
T = N/fs;
t = linspace(0,T,N);

B = reshape(Data(:,i),[N/T T]);
C = mean(B,2);
N2 = length(C);
T2 = N2/fs;
t2 = linspace(0,T2,N2);

G = [10000 1000 0];
persine = @(G,t2) G(1) + G(2)*sin(2*pi()*fp(j).*t2 + G(3));
[G2,fminres] = lsqcurvefit(persine,G,t2.',C);

Guess = G2(1) + G2(2)*sin(2*pi()*fp(j).*t2 + G2(3)) ;

Amp(j,i)= G2(2);
DC(j,i)= G2(1);
plot(t2,C,t2,Guess,'LineWidth',2)
xlim([0 1]);
end
end

for j = 1:k_max
measvol(j) = pi()/fp(j)*abs(Amp(j,2));
expvol(j)  = (Vref - ((1013+DC(j,1)-abs(Amp(j,1)))./(1013+DC(j,1)+abs(Amp(j,1)))...
             *Vref.^0.99346).^(1/0.99346))*1000000; %m3 to mL
K(j) = sqrt(expvol(j)./measvol(j));
end

plot(fp,[measvol expvol],'LineWidth',2)%
set(gca,'FontName','Arial','FontSize',12,'FontWeight','Bold','LineWidth',1)
%  ylim([0 40]);
    ylabel('{Volume per stroke[mL]}')
    legend('Measured volume','Calculated volume')
    xlabel('Frequency[hz]')
clc
save('S01_SS_K','K')
```

3. Code to calculate correction factors for pressure-sweep impedance

```
%% Time graphs
clear all; close all; clc
load('C:\Users\Frank\Desktop\M sorted Data - Rewrite\Matlab Data files\M0S_PS_6hz.mat')
A(1:6000,:) = R;
A = cat(3,A); % this 3 stands for 3rd dimension
clear R
fp = 6*ones(k_max,1);
IAP= linspace(1,20,20);

fs = 200;
Vref = 3.573/1000; % Inhoud ref impedance in mL

DC=zeros(k_max,2);
Amp=zeros(k_max,2);
measvol=zeros(k_max,1);
expvol=zeros(k_max,1);
K=zeros(k_max,1);
for j = 1:k_max
p_index     = ((j-1)*n_c)+3; % 3rd column in excel is pressure at the trocar

p2    = A(:,p_index);
p3    = A(:,p_index+1);
p4    = A(:,p_index+2);
% mean(K) = 1.0622 used for initial K
flow  = 1000./60.*(293.15./303.15).*((p3+1013.25)./1013.25)...
        .*1.0622.*sign(p3-p4).*sqrt(abs(p3-p4)); % Whitepaper Respironics
Data = [p2 flow];

for i = 1:2;
N = length(Data(:,i)); %
T = N/fs;
t = linspace(0,T,N);

B = reshape(Data(:,i),[N/T T]);
C = mean(B,2);
N2 = length(C);
T2 = N2/fs;
t2 = linspace(0,T2,N2);

G = [10000 1000 0];
persine = @(G,t2) G(1) + G(2)*sin(2*pi()*fp(j).*t2 + G(3));
[G2,fminres] = lsqcurvefit(persine,G,t2.',C);

Guess = G2(1) + G2(2)*sin(2*pi()*fp(j).*t2 + G2(3)) ;

Amp(j,i)= G2(2);
DC(j,i)= G2(1);
plot(t2,C,t2,Guess,'LineWidth',2)
xlim([0 1]);
end
end

for j = 1:k_max
measvol(j) = pi()/fp(j)*abs(Amp(j,2));
expvol(j)  = (Vref - ((1013+DC(j,1)-abs(Amp(j,1)))./(1013+DC(j,1)+abs(Amp(j,1)))...
             *Vref.^0.99346).^(1/0.99346))*1000000; %m3 to mL
K(j) = expvol(j)./measvol(j);
end

plot(IAP,[measvol expvol],'LineWidth',2)%
set(gca,'FontName','Arial','FontSize',12,'FontWeight','Bold','LineWidth',1)
    ylim([0 5]);
    ylabel('{Volume per stroke[mL]}')
    legend('Measured volume','Calculated volume')
    xlabel('pressure[hPa]')
clc
save('S01_PS_K','K')
```

4. Code to show properties forcing pressure signal, 1.4

```
%% Spectral estimator over entire measurements
close all; clear all; clc; tic

%% Load files
fp  = 6;    % [hz] select forcing pressure signal frequency
j   = 10;   % [hPa] select mean IAP used
W = 6;      % # of averages,

load('C:\Users\Frank\Desktop\M sorted Data - Rewrite\Matlab Data files\M03_PS_6hz_1.mat')
load('S01_PS_K.mat')
A = cat(3,R);
clear R

DATA = A(:,:,1);
fs=200;
p_index     = ((j-1)*n_c)+3;
p1          = DATA(:,p_index-1);% 2nd column pressure at manifold
p2          = DATA(:,p_index);  % 3rd column pressure at the trocar
p3          = DATA(:,p_index+1);% 4th column pressure manifold side sensor

Data = [p1 p3 p2];
WM_Spp_result  = zeros(250:3);
WM_freq_result = zeros(250:3);

for k = 1:3
    p= Data(:,k);
%% Spectral estimator, No Smoothing
NS_N = length(p); %
NS_T = NS_N/fs;
NS_freq = (1:NS_N/2).'/NS_T;

%% Spectral estimator, Welch Method
% reshape
WM_p=reshape(p,NS_N/W,W);

% windowing
w = window(@hann,length(WM_p));
WM_p = WM_p.*repmat(w,1,W);
WM_N = length(WM_p);
WM_T = WM_N/fs;

% input/pressure
WM_P = fft(WM_p);
WM_P = WM_P(2:WM_N/2+1,:);
WM_Spp_all = 1/WM_N*real(conj(WM_P).*WM_P);
WM_Spp = mean(WM_Spp_all,2);
WM_freq = (1:WM_N/2).'/WM_T;

WM_Spp_result(:,k)  = WM_Spp;
WM_freq_result(:,k) = WM_freq;
end

%% Surgical working space impedance, 5[s] time window and Welch
t = linspace(0,NS_T,NS_N);

figure(1)
subplot(2,1,1)
plot(t,Data,'LineWidth',2); hold on
plot([0 60],[mean(p2) mean(p2)],'k--','LineWidth',1);
set(gca,'FontName','Arial','FontSize',12,'FontWeight','Bold','LineWidth',1)
    legend({'manifold','flow sensor','trocar','mean'},'Location','northeast')
    xlim([15 16])
    ylim([0 20])
    ylabel('pressure [hPa]')
    xlabel('time [s]')

subplot(2,1,2)
```

```
plot(WM_freq_result(:,1),mag2db(WM_Spp_result),'LineWidth',2)
set(gca,'FontName','Arial','FontSize',12,'FontWeight','Bold','LineWidth',1)
    xlim([0 25])
    legend({'manifold','flow sensor','trocar'},'Location','northeast')
    ylabel('Amplitude [dB]')
    xlabel('frequency [hz]')

%% Display proces time
toc;
display('Total number of datapoints')
numel(A)
save('M01_PS_Results.mat')
```

5. Code to calculate impedance frequency-sweeps

```
%% Spectral estimator over entire measurements
close all; clear all; clc; tic
W = 12;
%% Load files
n_f = 4; % # of files that will be loaded
load('C:\Users\Frank\Desktop\M sorted Data - Rewrite\Matlab Data files\M02_SS_IAP10.mat')
B = R((1:12000),:);
load('C:\Users\Frank\Desktop\M sorted Data - Rewrite\Matlab Data files\M03_SS_IAP10.mat')
C = R((1:12000),:);
load('C:\Users\Frank\Desktop\M sorted Data - Rewrite\Matlab Data files\M04_SS_IAP10.mat')
D = R((1:12000),:);
load('C:\Users\Frank\Desktop\M sorted Data - Rewrite\Matlab Data files\M03_SS_IAP5.mat')
E = R((1:12000),:);
load('S01_SS_K.mat')
A = cat(3,B,C,D,E);

%% Setup parameters
WM_freq_result  = zeros(n_f,k_max);
WM_Hws_result   = zeros(n_f,k_max);
WM_C_result     = zeros(n_f,k_max);
WM_Rws_SD_result= zeros(n_f,k_max);
WM_Xws_SD_result= zeros(n_f,k_max);
WM_Rws_CV_result= zeros(n_f,k_max);
WM_Xws_CV_result= zeros(n_f,k_max);

for i = 1:n_f % select .mat file

DATA = A(:,:,i);

for j = 1:k_max
p_index     = ((j-1)*n_c)+3; % 3rd column in excel is pressure at the trocar
flow_index  = ((j-1)*n_c)+7; % 7nd column in excel is flow near the trocar
storz_index = ((j-1)*n_c)+11; % 11th column in excel is measured storz pressure

fp      = j+1;              % perturbation frequency
K_temp  = K(j);%mean(K);
p2    = DATA(:,p_index);
p3    = DATA(:,p_index+1);
p4    = DATA(:,p_index+2);
flow  = (293.15./303.15).*((p3+1013.25)./1013.25)...
        .*1.0622.*sign(p3-p4).*sqrt(abs(p3-p4)); % Whitepaper Respironics

    Data = [p2 flow];

%% Bandpass filtering for Perturbation signal
[b,a] = butter(4,[fp-1 fp+1]/(fs/2),'bandpass');
p_bp     = filtfilt(b,a,p2); % zero phase filter
flow_bp     = K_temp.*filtfilt(b,a,flow); % zero phase filter

%% Lowpass filtering for Perturbation signal
[b,a]   = butter(2,1.3/(fs/2),'low');
p_lp    = filtfilt(b,a,p2); % zero phase filter

%% Spectral estimator, No Smoothing
NS_N = length(p_bp); %
NS_T = NS_N/fs;
NS_freq = (1:NS_N/2).'/NS_T;

%% Spectral estimator, Welch Method

% reshape
WM_p_bp=reshape(p_bp,NS_N/W,W);
WM_flow_bp=reshape(flow_bp,NS_N/W,W);

% windowing
w = window(@hann,length(WM_p_bp));
WM_p_bp = WM_p_bp.*repmat(w,1,W);
```

```
WM_flow_bp = WM_flow_bp.*repmat(w,1,W);

WM_N = length(WM_p_bp);
WM_T = WM_N/fs;

% input/pressure
WM_P = fft(WM_p_bp);
WM_P = WM_P(2:WM_N/2+1,:);
WM_Spp_all = 1/WM_N*real(conj(WM_P).*WM_P);
WM_Spp = mean(WM_Spp_all,2);

% output/flow
WM_F = fft(WM_flow_bp);
WM_F = WM_F(2:WM_N/2+1,:);
WM_Sff_all= 1/WM_N*real(conj(WM_F).*WM_F);
WM_Sff = mean(WM_Sff_all,2);

% transfer
WM_Sfp_all =1/WM_N*conj(WM_P).*WM_F;
WM_Sfp=mean(WM_Sfp_all,2);

% estimator
WM_freq = (1:WM_N/2).'/WM_T;
WM_Hws  = WM_Sfp./WM_Spp;
WM_C    = abs(WM_Sfp).^2./(WM_Spp.*WM_Sff);
WM_Hws_all  = WM_Sfp_all./WM_Spp_all;

[~, index_wm] = min(abs(WM_freq-fp));
WM_Hws_all = WM_Hws_all(index_wm,:);

% confidence interval
WM_Rws_all = real(WM_Hws_all);
WM_Xws_all = imag(WM_Hws_all);
WM_Rws_mean= real(mean(WM_Hws_all,2));
WM_Xws_mean= imag(mean(WM_Hws_all,2));

WM_Rws_SD = (sum(((abs(WM_Rws_all-repmat(WM_Rws_mean,...
                    1,length(WM_Rws_all))).^2))/...
                    (length(WM_Rws_all)-1)).^(0.5));
WM_Xws_SD = (sum(((abs(WM_Xws_all-repmat(WM_Xws_mean,...
                    1,W)).^2))/...
                    (length(WM_Xws_all)-1)).^(0.5));

WM_Rws_CV = WM_Rws_SD./abs(WM_Rws_mean);
WM_Xws_CV = WM_Xws_SD./abs(WM_Xws_mean);

%% Lookup value at perturbation frequency

% find index
[~, WM_index] = min(abs(WM_freq-fp));

% Welch method
WM_freq_result(i,j) = WM_freq(WM_index);
WM_Hws_result(i,j)  = WM_Hws(WM_index);
WM_C_result(i,j)    = WM_C(WM_index);
WM_Rws_SD_result(i,j)= WM_Rws_SD;
WM_Xws_SD_result(i,j)= WM_Xws_SD;
WM_Rws_CV_result(i,j)= WM_Rws_CV;
WM_Xws_CV_result(i,j)= WM_Xws_CV;
end
end

%% Delete results from sample at 8hz and 19 hz(fp = j+1), in subject 2.
% These were not recorded and replaced with a dummy sample
RE    = real(WM_Hws_result);    RE(1,8) = nan;  RE(1,18) = nan;
IM    = imag(WM_Hws_result);    IM(1,8) = nan;  IM(1,18) = nan;
CPlot = WM_C_result;         CPlot(1,8) = nan; CPlot(1,18) = nan;
WM_Rws_CV_result(1,8) = nan; WM_Rws_CV_result(1,18) = nan;
WM_Xws_CV_result(1,8) = nan; WM_Xws_CV_result(1,18) = nan;

%% Surgical working space impedance, 5[s] time window and Welch
```

```
figure(1)
subplot(2,1,1)
        plot(WM_freq_result(1,:),RE((1:2),:),'LineWidth',2);hold on
        plot(WM_freq_result(1,:),RE(4,:),'--','LineWidth',2);hold on
        ylim([-1 10])
xlim([4 20])
ylabel('{R_{ws}[hPa\cdotmin/L]}')
        yyaxis right
        plot(WM_freq_result(1,:),RE(3,:),'LineWidth',2);hold on
        ylim([-1 10])
legend({'30[kg],subject 2','27[kg], subject 3','IAP 5[hPa], subject 3',...
        '38[kg], subject 4'},'Location','northeast')
set(gca,'FontName','Arial','FontSize',12,'FontWeight','Bold','LineWidth',1)

subplot(2,1,2)
set(gca,'FontName','Arial','FontSize',12,'FontWeight','Bold','LineWidth',1)

        plot(WM_freq_result(1,:),IM((1:2),:),'LineWidth',2);hold on
        plot(WM_freq_result(1,:),IM(4,:),'--','LineWidth',2);hold on
        ylim([-20 0])
xlim([4 20])
ylabel('{X_{ws}[hPa\cdotmin/L]}')
xlabel('frequency [hz]')
        yyaxis right
        plot(WM_freq_result(1,:),IM(3,:),'LineWidth',2);hold on
        ylim([-5  0])
set(gca,'FontName','Arial','FontSize',12,'FontWeight','Bold','LineWidth',1)

%% Coefficient of variation
figure(2)
colormap lines(4)
subplot(2,1,1);
    bar(WM_freq_result(1,:),WM_Rws_CV_result.','BarWidth',0.97,'EdgeColor','none');hold on
subplot(2,1,2);
    bar(WM_freq_result(1,:),WM_Xws_CV_result.','BarWidth',0.97,'EdgeColor','none');hold on
subplot(2,1,1);
set(gca,'FontName','Arial','FontSize',12,'FontWeight','Bold','LineWidth',1)
    ylabel('{CV R_{ws}[-]}')
    ylim([0 0.5])
    xlim([3.5 20.5])
        legend({'30[kg],subject 2','27[kg], subject 3','38[kg], subject 4',...
        'IAP 5 [hPa], subject 3'},'Location','northeast')
subplot(2,1,2);
set(gca,'FontName','Arial','FontSize',12,'FontWeight','Bold','LineWidth',1)
    ylabel('{CV X_{ws}[-]}')
    ylim([0 0.5])
    xlabel('frequency [hz]')
    xlim([3.5 20.5])

%% Display proces time
toc;
display('Total number of datapoints')
numel(A)
save('M99SS_Results.mat')
```

6. Code to calculate impedance pressure-sweeps

```
%% Spectral estimator over entire measurements
close all; clear all; clc; tic
W = 12;
%% Load files
n_f = 4; % # of files that will be loaded
load('C:\Users\Frank\Desktop\M sorted Data - Rewrite\Matlab Data files\M03_PS_6hz_5.mat')
E = R; %% Largest file, most mean IAP levels used
B = nan(size(E)); C=B; D=B;
load('C:\Users\Frank\Desktop\M sorted Data - Rewrite\Matlab Data files\M02_PS_6hz_1.mat')
B((1:12000),(1:210)) = R((1:12000),:);
load('C:\Users\Frank\Desktop\M sorted Data - Rewrite\Matlab Data files\M03_PS_6hz_1.mat')
C((1:12000),(1:280)) = R((1:12000),:);
load('C:\Users\Frank\Desktop\M sorted Data - Rewrite\Matlab Data files\M04_PS_6hz_1.mat')
D((1:12000),(1:280)) = R((1:12000),:);
clear R
load('S01_PS_K.mat')
A = cat(3,B,C,D,E);
IAP = linspace(1,25,25);
k_max=25;
K = [K;K(10);K(10);K(10);K(10);K(10)];
%% Setup parameters
WM_freq_result  = zeros(n_f,k_max);
WM_Hws_result   = zeros(n_f,k_max);
WM_C_result     = zeros(n_f,k_max);
WM_Rws_SD_result= zeros(n_f,k_max);
WM_Xws_SD_result= zeros(n_f,k_max);
WM_Rws_CV_result= zeros(n_f,k_max);
WM_Xws_CV_result= zeros(n_f,k_max);

for i = 1:n_f % select .mat file
DATA = A(:,:,i);

for j = 1:k_max
p_index     = ((j-1)*n_c)+3; % 3rd column in excel is pressure at the trocar
storz_index = ((j-1)*n_c)+11; % 11th column in excel is measured storz pressure

fp      = 6;              % perturbation frequency
K_temp  = K(j);%mean(K);
p2    = DATA(:,p_index);
p3    = DATA(:,p_index+1);
p4    = DATA(:,p_index+2);
flow  = (293.15./303.15).*((p3+1013.25)./1013.25)...
        .*1.0622.*sign(p3-p4).*sqrt(abs(p3-p4)); % Whitepaper Respironics
Data = [p2 flow];

%% Bandpass filtering for Perturbation signal
[b,a] = butter(4,[fp-1 fp+1]/(fs/2),'bandpass');
p_bp     = filtfilt(b,a,p2); % zero phase filter
flow_bp     = K_temp.*filtfilt(b,a,flow); % zero phase filter

%% Lowpass filtering for Perturbation signal
[b,a]   = butter(2,1.3/(fs/2),'low');
p_lp    = filtfilt(b,a,p2); % zero phase filter

%% Spectral estimator, No Smoothing
NS_N = length(p_bp); %
NS_T = NS_N/fs;
NS_freq = (1:NS_N/2).'/NS_T;

%% Spectral estimator, Welch Method

% reshape
WM_p_bp=reshape(p_bp,NS_N/W,W);
WM_flow_bp=reshape(flow_bp,NS_N/W,W);

% windowing
w = window(@hann,length(WM_p_bp));
```

```
WM_p_bp = WM_p_bp.*repmat(w,1,W);
WM_flow_bp = WM_flow_bp.*repmat(w,1,W);

WM_N = length(WM_p_bp);
WM_T = WM_N/fs;

% input/pressure
WM_P = fft(WM_p_bp);
WM_P = WM_P(2:WM_N/2+1,:);
WM_Spp_all = 1/WM_N*real(conj(WM_P).*WM_P);
WM_Spp = mean(WM_Spp_all,2);

% output/flow
WM_F = fft(WM_flow_bp);
WM_F = WM_F(2:WM_N/2+1,:);
WM_Sff_all= 1/WM_N*real(conj(WM_F).*WM_F);
WM_Sff = mean(WM_Sff_all,2);

% transfer
WM_Sfp_all =1/WM_N*conj(WM_P).*WM_F;
WM_Sfp=mean(WM_Sfp_all,2);

% estimator
WM_freq = (1:WM_N/2).'/WM_T;
WM_Hws  = WM_Sfp./WM_Spp;
WM_C    = abs(WM_Sfp).^2./(WM_Spp.*WM_Sff);
WM_Hws_all  = WM_Sfp_all./WM_Spp_all;

[~, index_wm] = min(abs(WM_freq-fp));
WM_Hws_all = WM_Hws_all(index_wm,:);

% confidence interval
WM_Rws_all = real(WM_Hws_all);
WM_Xws_all = imag(WM_Hws_all);
WM_Rws_mean= real(mean(WM_Hws_all,2));
WM_Xws_mean= imag(mean(WM_Hws_all,2));

WM_Rws_SD = (sum(((abs(WM_Rws_all-repmat(WM_Rws_mean,...
                    1,length(WM_Rws_all))).^2))/...
                    (length(WM_Rws_all)-1)).^(0.5));
WM_Xws_SD = (sum(((abs(WM_Xws_all-repmat(WM_Xws_mean,...
                    1,W)).^2))/...
                    (length(WM_Xws_all)-1)).^(0.5));

WM_Rws_CV = WM_Rws_SD./abs(WM_Rws_mean);
WM_Xws_CV = WM_Xws_SD./abs(WM_Xws_mean);

%% Lookup value at perturbation frequency

% find index
[~, WM_index] = min(abs(WM_freq-fp));

% Welch method
WM_freq_result(i,j) = WM_freq(WM_index);
WM_Hws_result(i,j)  = WM_Hws(WM_index);
WM_C_result(i,j)    = WM_C(WM_index);
WM_Rws_SD_result(i,j)= WM_Rws_SD;
WM_Xws_SD_result(i,j)= WM_Xws_SD;
WM_Rws_CV_result(i,j)= WM_Rws_CV;
WM_Xws_CV_result(i,j)= WM_Xws_CV;
end
end

RE    = real(WM_Hws_result);
IM    = imag(WM_Hws_result);
CPlot = WM_C_result;

%% Surgical working space impedance, 5[s] time window and Welch
figure(1)
subplot(2,1,1)
        plot(IAP,RE((1:2),:),'LineWidth',2);hold on
```

```
        plot(IAP,RE(4,:),'--','LineWidth',2);hold on
        ylim([-1 20])
xlim([0 25])
ylabel('{R_{ws}[hPa\cdotmin/L]}')
        yyaxis right
        plot(IAP,RE(3,:),'LineWidth',2);hold on
        ylim([-1 5])
legend({'30[kg],subject 2','27[kg], subject 3','extended, subject 3',...
        '38[kg], subject 4'},'Location','northwest')
set(gca,'FontName','Arial','FontSize',12,'FontWeight','Bold','LineWidth',1)

subplot(2,1,2)
set(gca,'FontName','Arial','FontSize',12,'FontWeight','Bold','LineWidth',1)

        plot(IAP,IM((1:2),:),'LineWidth',2);hold on
        plot(IAP,IM(4,:),'--','LineWidth',2);hold on
        ylim([-10 1])
xlim([0 25])
ylabel('{X_{ws}[hPa\cdotmin/L]}')
xlabel('pressure [hPa]')
        yyaxis right
        plot(IAP,IM(3,:),'LineWidth',2);hold on
        ylim([-0.5  0.05])
set(gca,'FontName','Arial','FontSize',12,'FontWeight','Bold','LineWidth',1)

%% Coefficient of variation
figure(2)
colormap lines(4)
subplot(2,1,1);
    bar(IAP,[WM_Rws_CV_result((1:2),:).' WM_Rws_CV_result(4,:).'...
        WM_Rws_CV_result(3,:).'],'BarWidth',0.97,'EdgeColor','none')
subplot(2,1,2);
    bar(IAP,[WM_Xws_CV_result((1:2),:).' WM_Xws_CV_result(4,:).'...
        WM_Xws_CV_result(3,:).'],'BarWidth',0.97,'EdgeColor','none')
subplot(2,1,1);
legend({'30[kg],subject 2','27[kg], subject 3','extended, subject 3',...
        '38[kg], subject 4'},'Location','northeast')
set(gca,'FontName','Arial','FontSize',12,'FontWeight','Bold','LineWidth',1)
    ylabel('{CV R_{ws}[-]}')
    ylim([0 1])
    xlim([0.5 25.5])
subplot(2,1,2);
set(gca,'FontName','Arial','FontSize',12,'FontWeight','Bold','LineWidth',1)
    ylabel('{CV X_{ws}[-]}')
    ylim([0 1])
    xlabel('pressure [hPa]')
    xlim([0.5 25.5])

 %% Coefficient of variation (not used)
% figure(3)
% colormap lines(4)
% subplot(2,1,1)
% errorbar(IAP,RE(4,:),2.*WM_Rws_SD_result(4,:),'LineWidth',2); hold on
% xlim([0.7 25.3])
% ylabel('{R_{ws}[hPa\cdotmin/L]}')
% legend({'30[kg],subject 2','27[kg], subject 3','extended, subject 3',...
%         '38[kg], subject 4'},'Location','northwest')
% set(gca,'FontName','Arial','FontSize',12,'FontWeight','Bold','LineWidth',1)
% subplot(2,1,2)
% errorbar(IAP,IM(4,:),2.*WM_Xws_SD_result(4,:),'LineWidth',2); hold on
% xlim([0.7 25.3])
% ylabel('{X_{ws}[hPa\cdotmin/L]}')
% xlabel('pressure [hPa]')
% set(gca,'FontName','Arial','FontSize',12,'FontWeight','Bold','LineWidth',1)

%% Display proces time
toc;
display('Total number of datapoints')
numel(A)
save('M99_PS_Results.mat')
```

C

Appendix: Labview code

1. Explanation User Interface

1.1. Current interface

The current generation of insufflation, like the Storz Endoflator 50 and the Stryker Pneumosure have a relatively simple interface. Previous generations only showed numerical values. Currently there are two main modes. Control mode provides four settings, pressure, flow, patient-mode and the on/off button. The pressure and flow bar present both the settings and current value on top of one another. The patient mode can be set to pediatric or adult, this changes the alarm settings. The on/off button is used to start insufflating or pause during insufflation.
Alarms are also presented in control mode. Alarms are presented in a bar in top of the screen. The amount of CO2 used during the procedure is presented separately, sometime the gas cylinder has to be replaced during surgery. The setting mode is used to change unit and alarm settings.

Figure C.1: The Karl Storz Endoflator 50

1.2. Labview conversion

The experimental setup uses Labview for recording of the signals. It makes sense then to use Labview for creating the user interface. The control mode is the most important mode for the surgeon. In the Erasmus MC only Storz Endoflators are used, this interface was recreated in Labview.
A few changes have been made when compared to the Karl Storz interface. The pressure and flow bars have different colours, this makes it easier to distinguish them. The measured value and settings are display side by side below the corresponding bar. The up and down buttons are enlarged and put to next to the corresponding bar, within a container to prevent confusion. The patient mode and CO2 measurements are put entirely to the right. An additional stop-button has been added to stop the entire virtual instrument. Errors are not shown, no communication protocol was available, reverse engineering every alarms code was to cumbersome. The settings will be discussed later, not all settings can be changed through the communication bus.

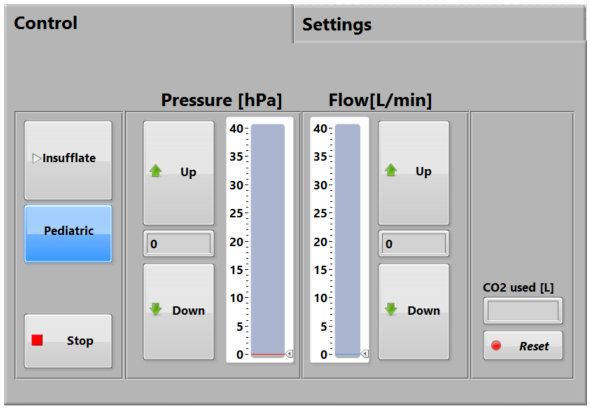

Figure C.2: Storz interface converted into Labview interface

1.3. Measurement interface

A third tab was added to the interface for control during the measurements. In the left top corner the FOT button can be used to turn the perturbation signal on and off. Below this button there is the reactance bar, it show the reactance at the perturbation frequency. The stop-button can be used to stop the entire virtual instrument. The large graph in the middle of the screen presents all the measurements obtained through the NI DAQMX. Four pressure-sensors were connected, in pairs. Each pair could also be used for flow measurements. In the current setup, pressure sensor 1 and 2 were used for actual pressure-measurements. The 3rd and 4th sensor were used for measuring the flow.
The left bottom graph was used to present the perturbation signal after bandpass-filtering. In the current setup this was a bandpass-filter applied to pressure 2, the pressure at the trocar. In the right bottom graph, the pressure measurement and settings by the insufflator where presented. These are sampled using a very low sample frequency, therefore a small graph was enough to detect changes. On the right there are two more buttons. On is for increasing or decreasing the perturbation frequency, in-between there is the actual perturbation frequency. The last button is for storing the data obtained during the pre-set time-window. The pressure calibration button enables the calibration curve from voltage to pressure in hPa.
The last tab can be used to change general settings. The leftmost column is used for insufflator settings. The COM-port for the Karl Storz Endoflator can be selected. It also displays the initialization steps. Custom messages can be send to the insufflator, this is useful for reverse engineering the communication protocol or enable/disable the output of certain parameters. The middle column involves all settings for the data acquisition and analysis. The pressure calibration can be turned of, then only the voltage from the pressure sensors is displayed and flow measurements are disabled. The auto-zero buttons can be used to zero the pressure or flow, this is most useful to prevent a bias in the flow measurements. The three counter can be used to verify if the virtual instrument is obtaining data. The gas-type used can be changed, the pressure and flow sensors can be used for air, pure oxygen and carbon dioxide. A second order low-pass filter is used to suppress the high frequency noise from the data acquisition, it can be set to FIR, IR or off. Finite impulse response is the most accurate filter, but it requires more computational effort. The Infinite Impulse filtering option was added in case a lower computational effort would be required. The analysing time can be changed, now a 5[s] is used, similar to the Welch method used in the matlab file. The second time window, t_I, is used for recording the samples. It was set to 6[s] in the pressure sweeps and 120[s] in the sine sweeps. In third column the entire output array is shown for reverse engineering the communication protocol.

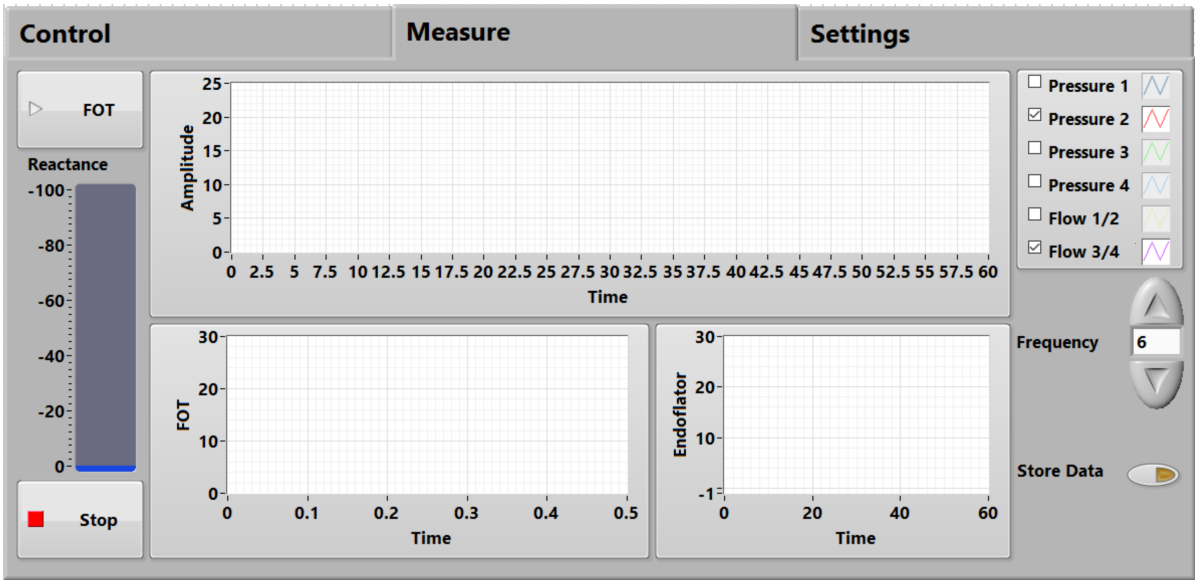

Figure C.3: Measurement monitoring panel Labview Interface

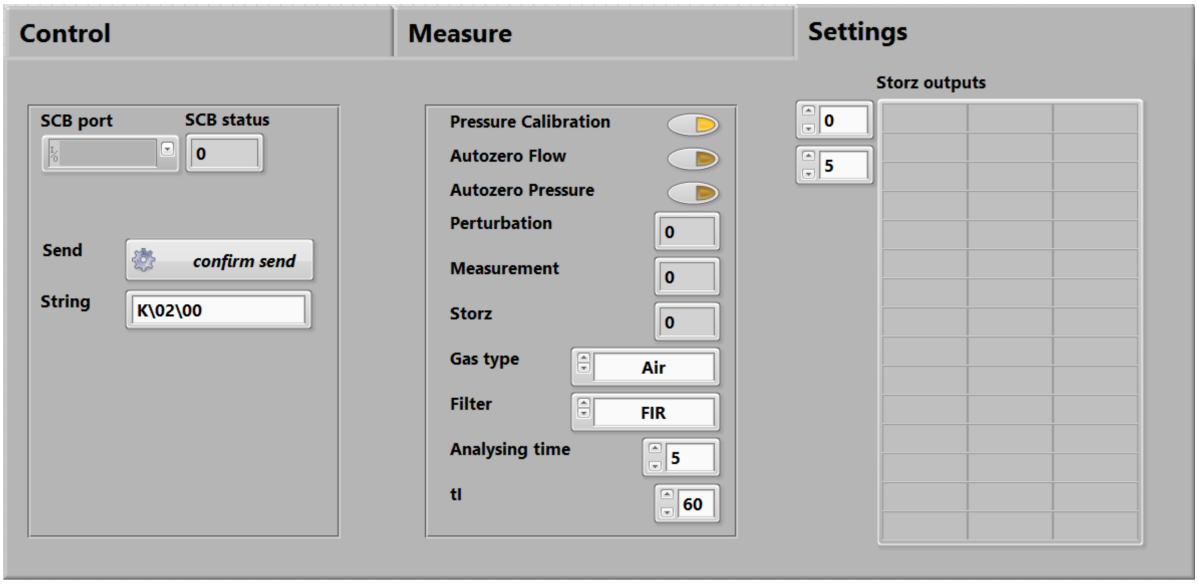

Figure C.4: Measurement settings panel Labview Interface

1.4. Future interface

The user interface for insufflation in combination with EndoFOT monitoring could be created by just adding the reactance bar indicator from the measurements tab. All alarms could be integrated into the general alarm system. For automated control other buttons and settings should be added. This is outside the scope of this research. An impression of a future interface for just monitoring of surgical workings space compliance is given in figure C.5.

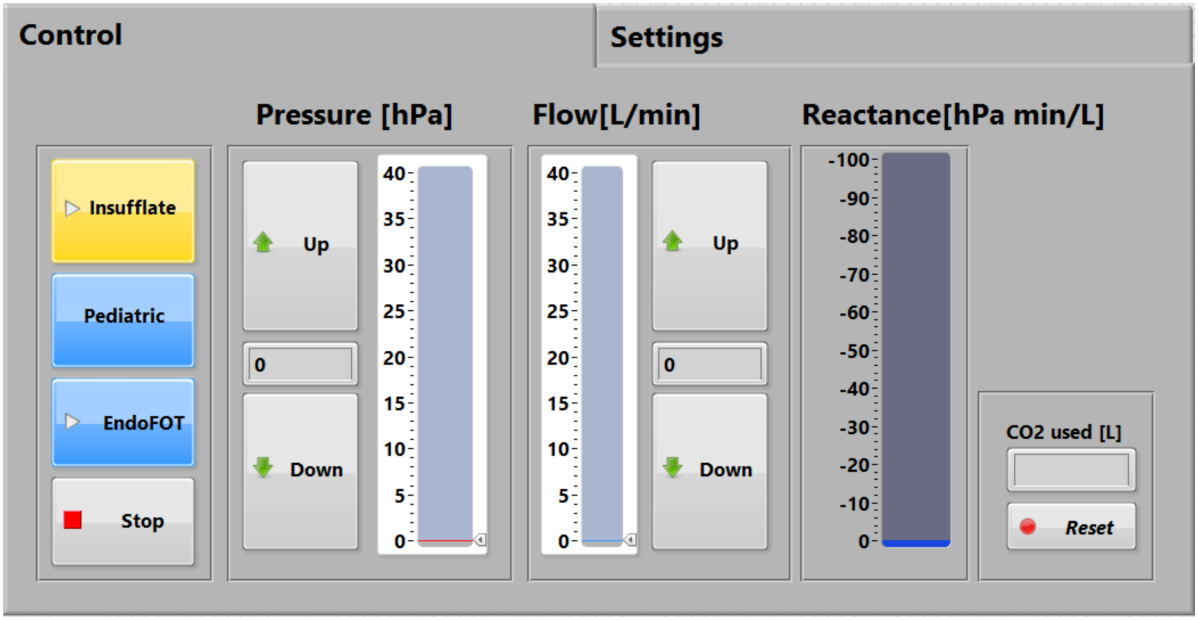

Figure C.5: Measurement settings panel Labview Interface

2. Code

2.1. Brief explanation main instrument

The virtual instrument is divided in to six successive frames. The first frame opens a visa connection for communication with the SCB, Storz Communication Bus. It is used to send and recieve data to/from the insufflator. Aside from opening other initializations take place. File-paths for errorlog files are created. Also important, global variables are declared to control the insufflator. The second frame initializes the time counter, it is used for data-synchronization purposes.

The third frame only beholds a sub-VI. This vi is used to initialize a connection between labview and the insufflator. The parameter output requires every parameter to be requested from the SCB. This sub-vi goes through seven steps starting at zero, it creates a log file at every startup and writes the error into it when initialization fails. The indicator can be used to verify the last step, step 6, is reached.

The fourth frame is used for multiple tasks. The files for data storage are created. Connection to the DAQMX for data acquisition is initialized. The variables and timers for the SCB-loop are created. And a connection to the audio hardware of the PC is made, the perturbation signal is created using audio signals.

The fifth frame is the most important frame. It both the perturbation and measurement loops. Data acquisistion from the DAQMX and SCB are within the same loop because they run at the same speed. The perturbation loop was allowed unlimited speed, it is controlled by Labview's vi for creating sound signals. Both loops are stopped simultaneous. The small perturbation loop is located at the bottom. It consist out of an tone generator and a true false box for turning on and of the speaker.

The lower part of the measurement loop is used for the insufflator. The while loop runs until all data is sorted and put into an array. The for loop is used to scan for every parameter. After this loop there is a set of indicators for the graphical user interface. Above these indicator there is an event box. It responds to control changes from the user interface and sends the appropriate commands to the insufflator.

The upper half of the measurement loop is used for the DAQMX. it startst with a 4-channel 100 samples waveform. This waveform contains the voltages originating from the pressure transducers. The first sub-vi is used for converting the voltages to pressures using the calibration curves. The correct curve is chosen by setting the gas type. The same goes for the flow. When using the waveform type, it is possible to assign labels to the created channels. This is also done within the same sub-VI. The perturbation frequency is added to the label of the first pressure sensor. Also the 30[hz] low-pass filter is applied in this sub-VI, hence the filter option. This sub-VI results in a 6-channel waveform including pressure and flow.

After this sub-VI all waveforms get re-sampled to 200[hz] and afterwards a buffer-VI is used combine all samples into a long waveform. The length of this waveform depends on the t_I-settings, usually this is 60 or120[s]. The insufflator array is used in a similar way. This is the waveform just above the DAQMX waveform. The Storz output array is resampled and labeled before relevant measurements are put in a similar buffer.

The third large waveform array contains the results of the frequency analysis done in Labview, just for real time presentation. The results shown in appendix D are obtained using matlab, because it is more suitable for creating graphs. This Sub-VI uses the DAQMX 6-channel waveform. A bandpass-filter is used to get rid of all frequencies outside a 1[hz] radius from the perturbation signal. Pressure 2 is compared to flow obtained using pressure sensor 3/4. The analysing time is used to for the time-window, it was set to 5[s]. After applying a Hanning window the Frequency response function was calculated. In Labview, the result was exponentially averaged over the last 100 estimations. The real part and imaginary part of the FRF at the perturbation frequency are re-sampled, labeled buffered for storage. This is the last sub-VI within the measurement loop. The three waveform arrays are combined, when the store button is pressed in the GUI. Every sample has a number and is stored within a time-stamped folder.

The very last frame is used for closing the VI. It disconnects the SCB, DAQMX and Audio-hardware. The next section contains the diagrams of this VI. The main VI, analysis VI and DAQMX VI are included in the following sections.

3. Main instrument code

Block Diagram

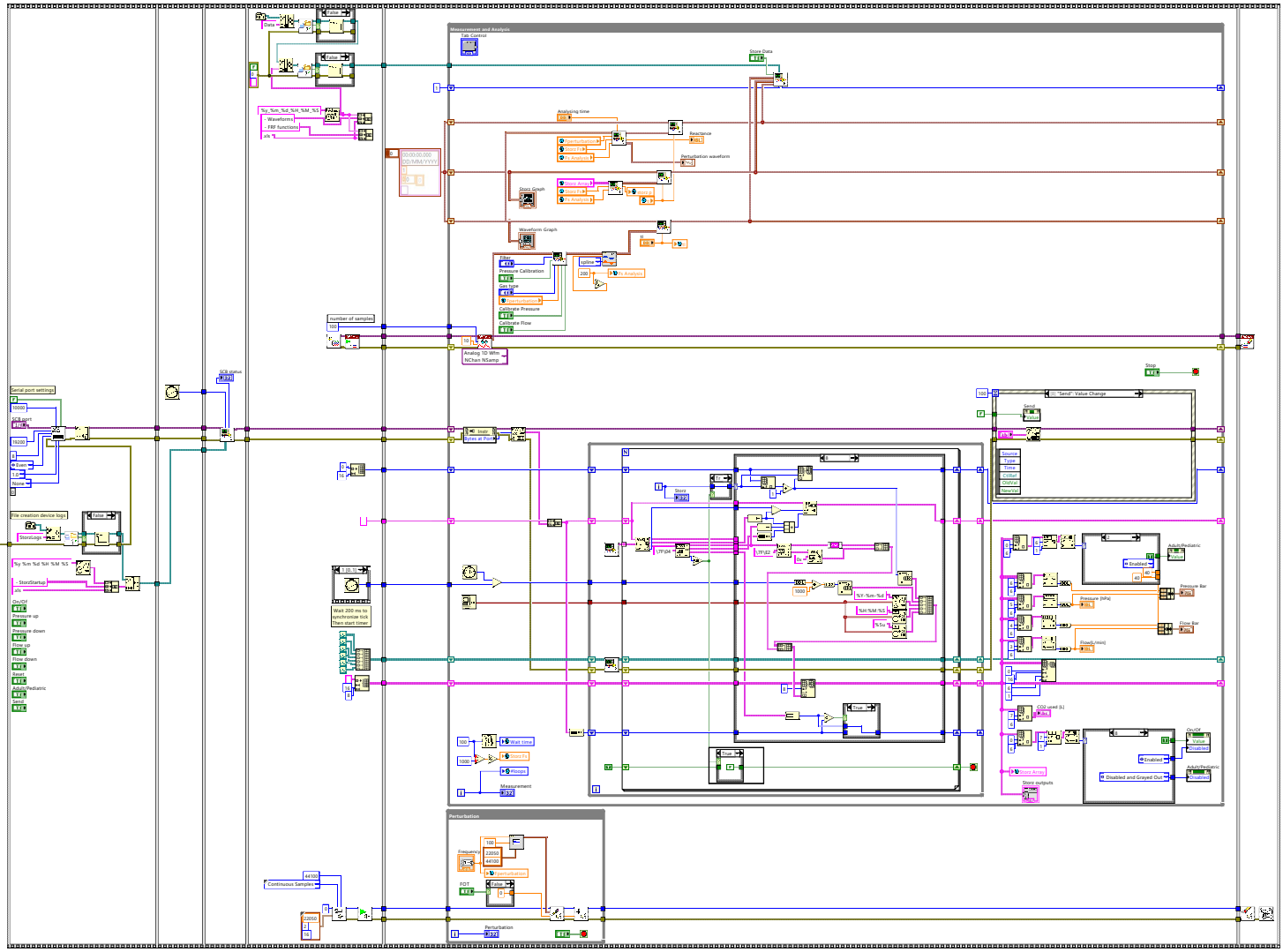

4. Code for Data Acquisition

Block Diagram

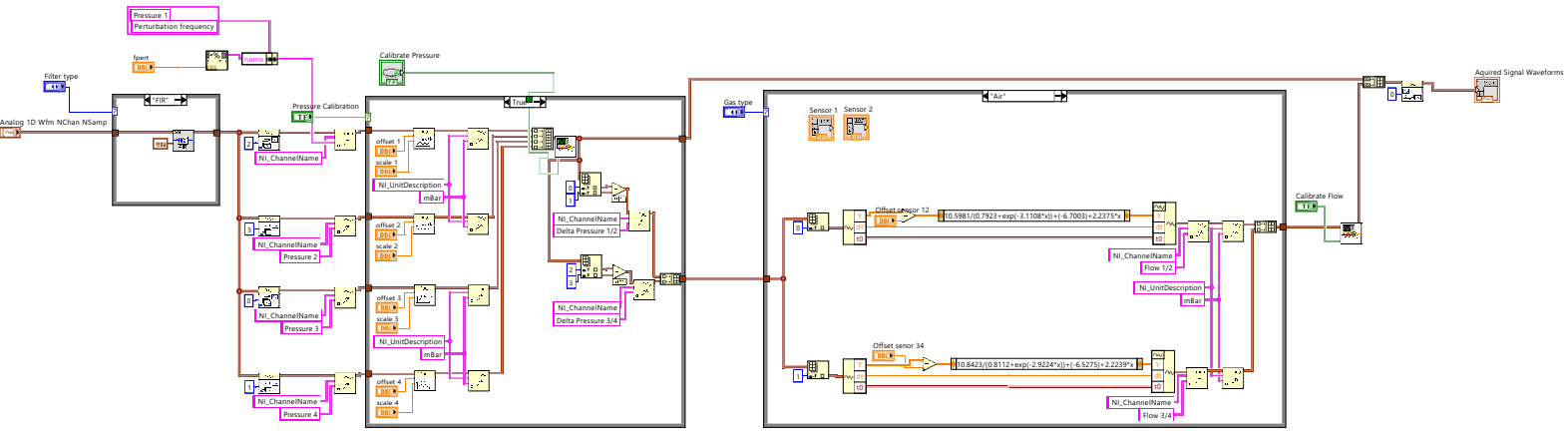

5. Code for real time EndoFOT analysis

Block Diagram

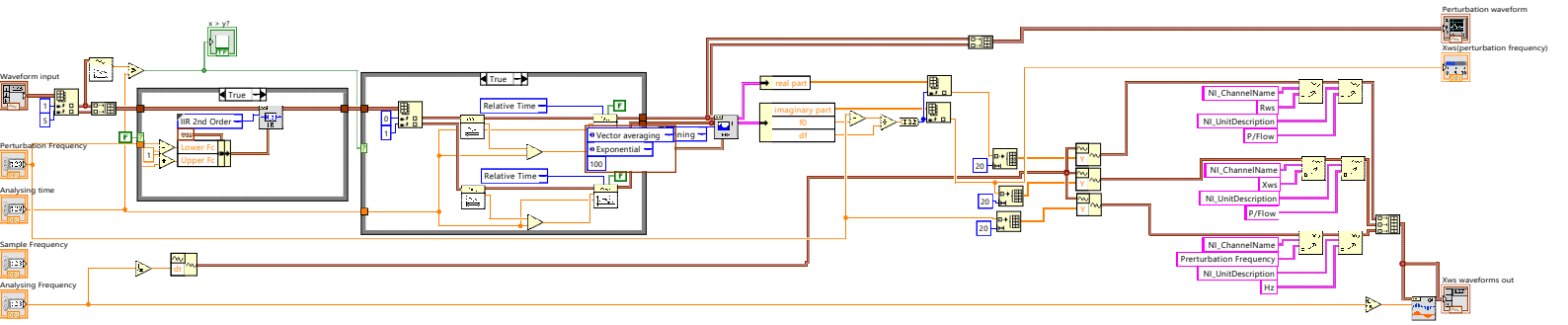

6. Code for connecting with Storz Communication Bus

Block Diagram

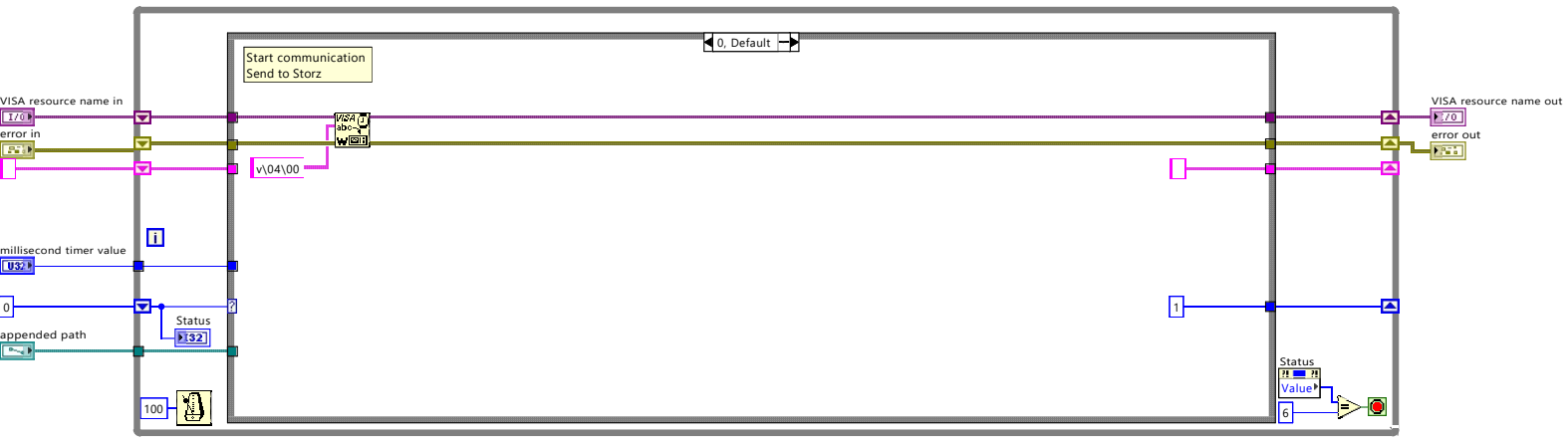

D

Appendix: Results

1. Subjects

Subject	Weight[kg]	IAP[hPa]	p_{EEP}[hPa]	p_{IP}[hPa]	V_{tidal}([L])	T_{resp}([s])	I:E [-]	notes
1	65	5,10 and 15	-	-	-	-	-	Post-mortem
2	30	1-15	5	16	0.223	2.7	1:3	In-vivo
3	27	1-20	5	19	0.278	2.5	1:2.9	In-vivo
4	38	1-20	4	24	0.500	2.7	1:1,7	In-vivo

Table D.1: List of subjects, their physical characteristics, used intra-abdominal pressures(IAP) and mechanical ventilator settings.

2. Subject #01, postmortem

2.1. Frequency sweeps

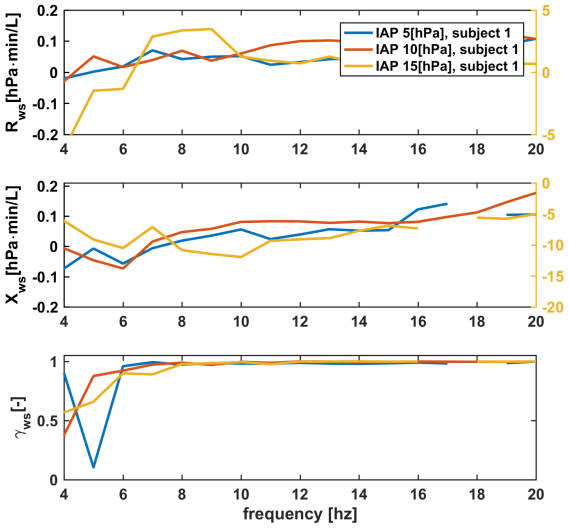

Figure D.1: Resistance, reactance and coherence during frequency sweeps in post-mortem subject at 5, 10 and 15 hPa of mean IAP.

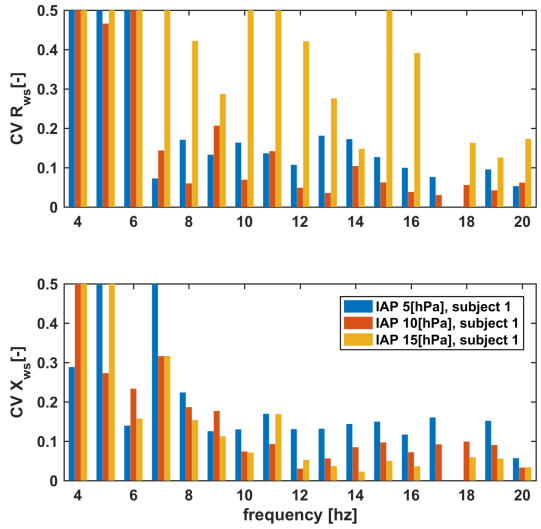

Figure D.2: Coefficients of variation in frequency sweeps in post-mortem subject at 5, 10 and 15 hPa of mean IAP.

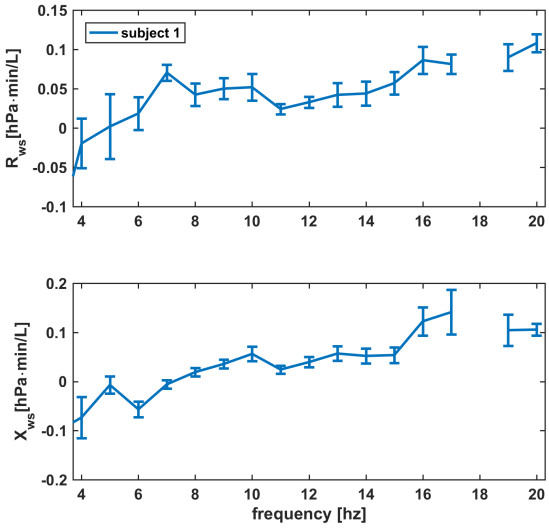

Figure D.3: Resistance, reactance and their 95% confidence intervals of frequency sweep in post-mortem subject at 5 hPa of mean IAP.

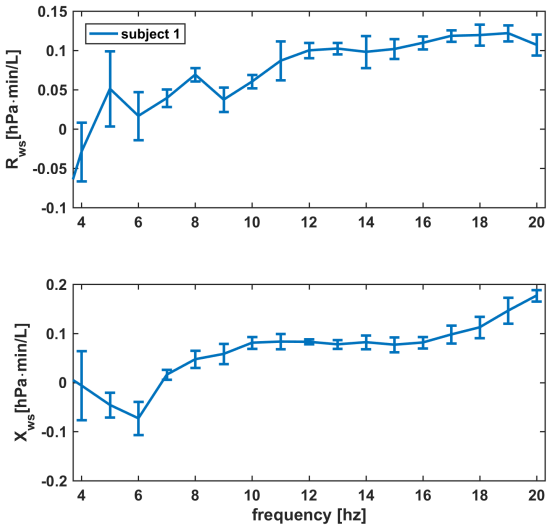

Figure D.4: Resistance, reactance and their 95% confidence intervals of frequency sweep in post-mortem subject at 10 hPa of mean IAP.

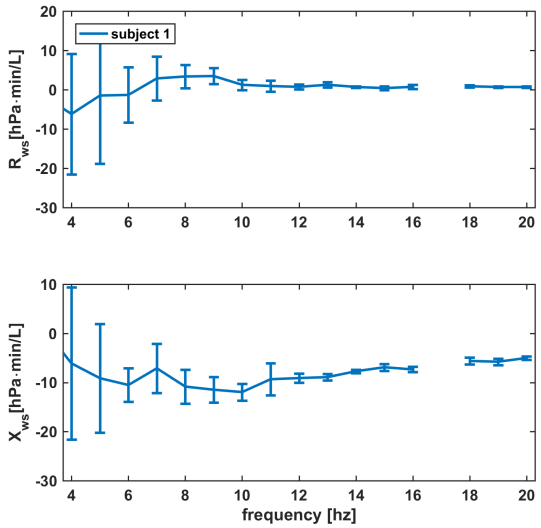

Figure D.5: Resistance, reactance and their 95% confidence intervals of frequency sweep in post-mortem subject at 15 hPa of mean IAP.

3. Subject #02, in-vivo

3.1. Frequency sweeps

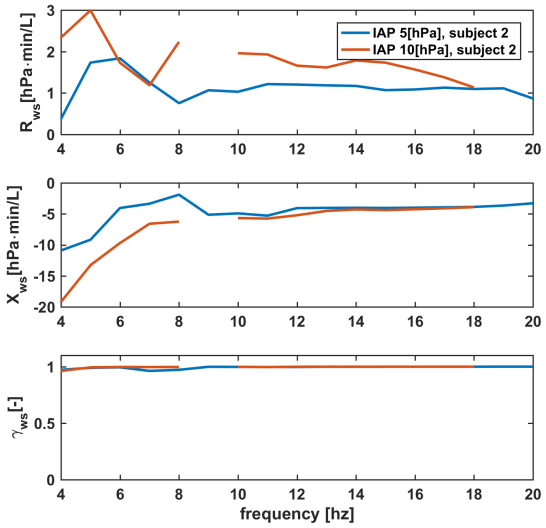

Figure D.6: Resistance, reactance and coherence during frequency sweeps in subject 2 at 5 and 10 hPa of mean IAP.

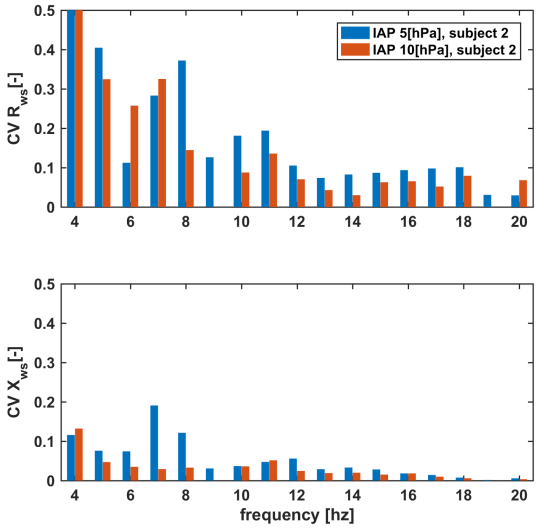

Figure D.7: Coefficients of variation in frequency sweeps in subject 2 at 5 and 10 hPa of mean IAP.

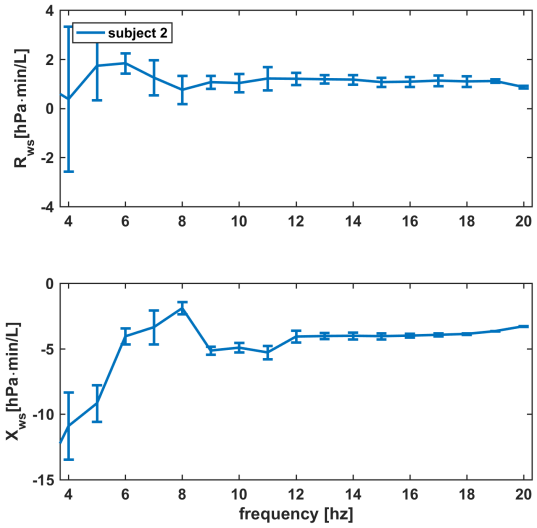

Figure D.8: Resistance, reactance and their 95% confidence intervals of frequency sweep in subject 2 at 5 hPa of mean IAP.

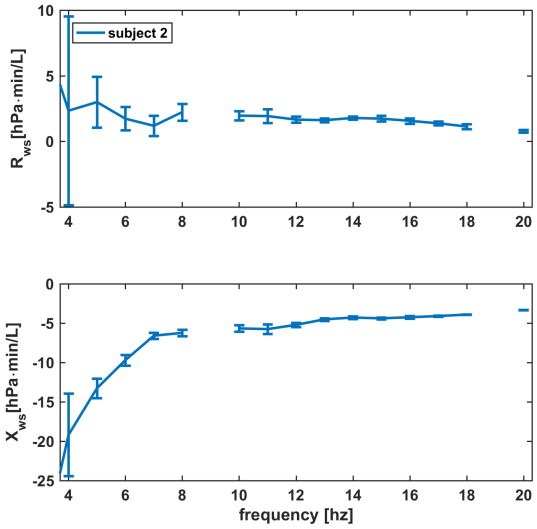

Figure D.9: Resistance, reactance and their 95% confidence intervals of frequency sweep in subject 2 at 10 hPa of mean IAP.

3.2. Pressure sweeps

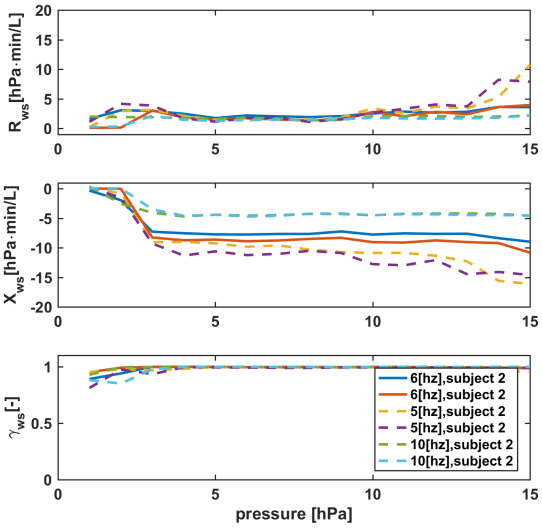

Figure D.10: Resistance, reactance and coherence during pressure sweeps in subject 2 at 5, 6 and 10 Hz.

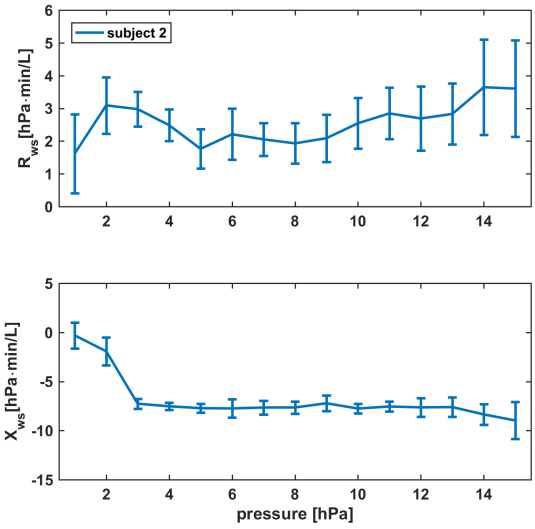

Figure D.12: Resistance, reactance and confidence intervals during pressure sweep in subject 2 at 6 Hz.

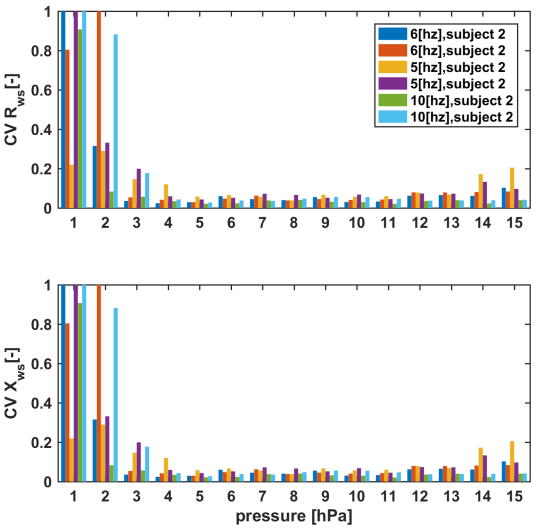

Figure D.11: Coefficients of variation in pressure sweeps in subject 2 at 5, 6 and 10 Hz.

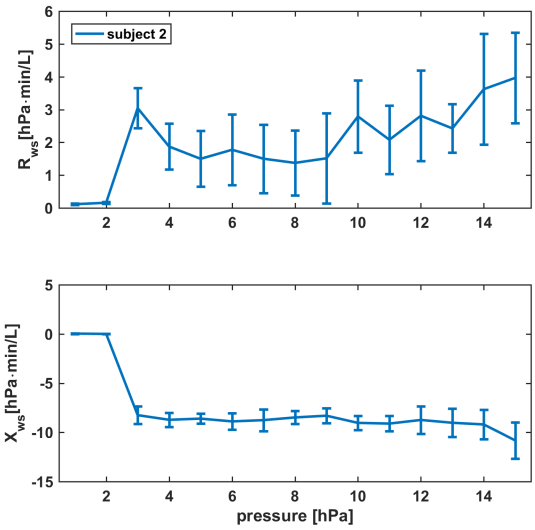

Figure D.13: Resistance, reactance and confidence intervals during pressure sweep in subject 2 at 6 Hz.

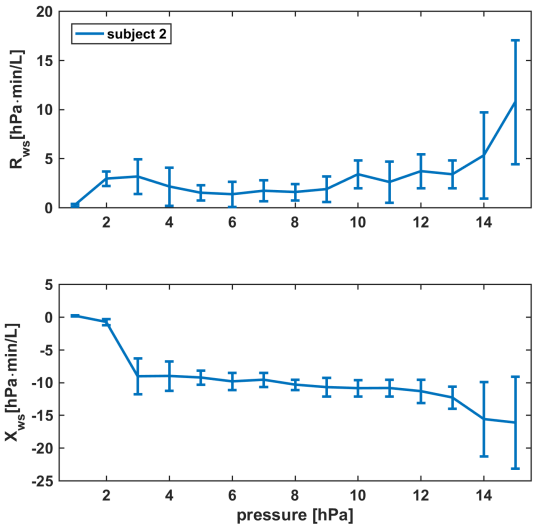

Figure D.14: Resistance, reactance and confidence intervals during pressure sweep in subject 2 at 5 Hz.

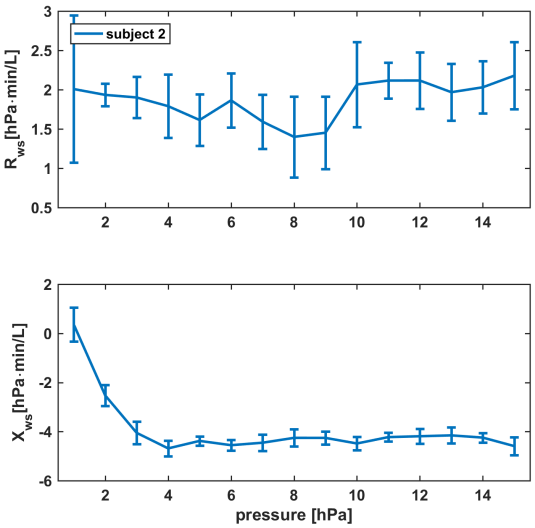

Figure D.16: Resistance, reactance and confidence intervals during pressure sweep in subject 2 at 10 Hz.

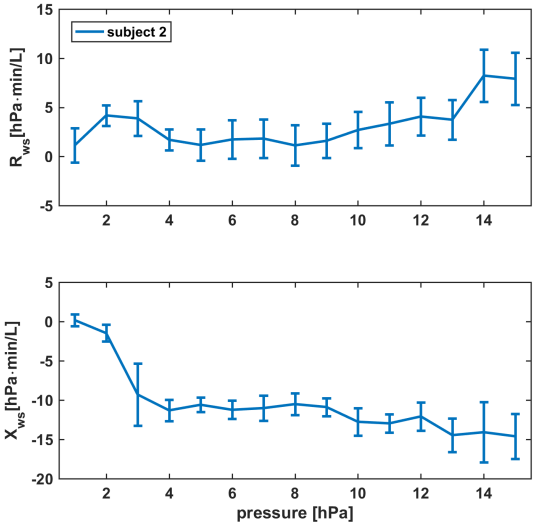

Figure D.15: Resistance, reactance and confidence intervals during pressure sweep in subject 2 at 5 Hz.

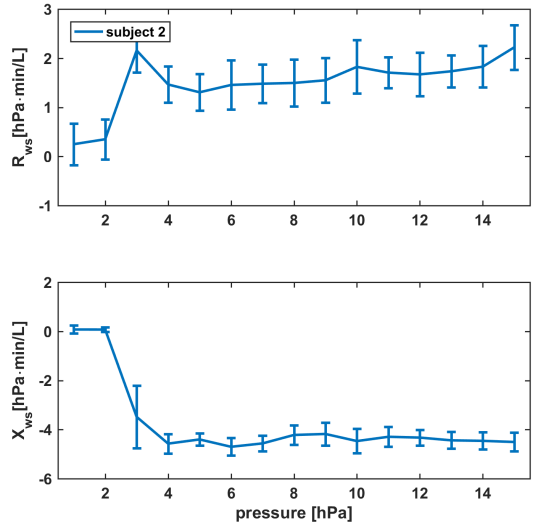

Figure D.17: Resistance, reactance and confidence intervals during pressure sweep in subject 2 at 10 Hz.

4. Subject #03, in-vivo

4.1. Frequency sweeps

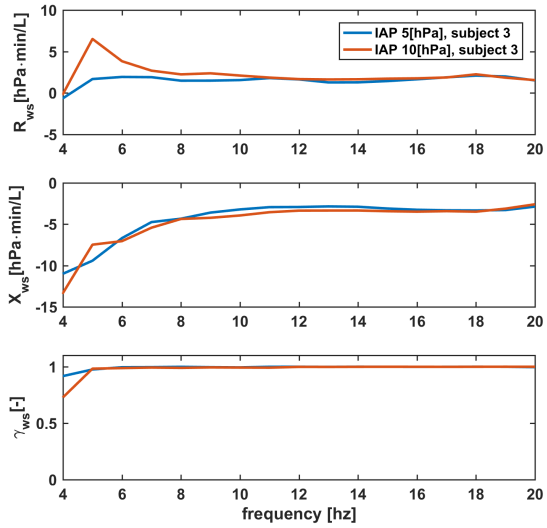

Figure D.18: Resistance, reactance and coherence during frequency sweeps in subject 3 at 5 and 10 hPa of mean IAP.

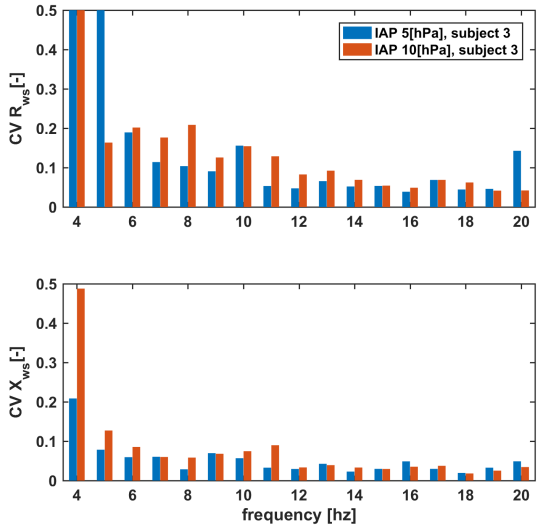

Figure D.19: Coefficients of variation in frequency sweeps in subject 3 at 5 and 10 hPa of mean IAP.

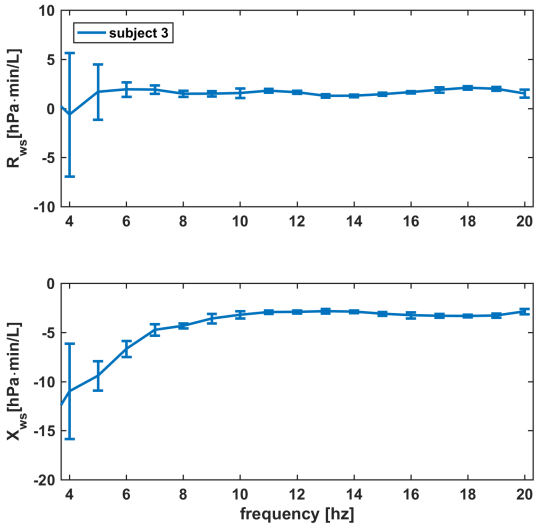

Figure D.20: Resistance, reactance and their 95% confidence intervals of frequency sweep in subject 3 at 5 hPa of mean IAP.

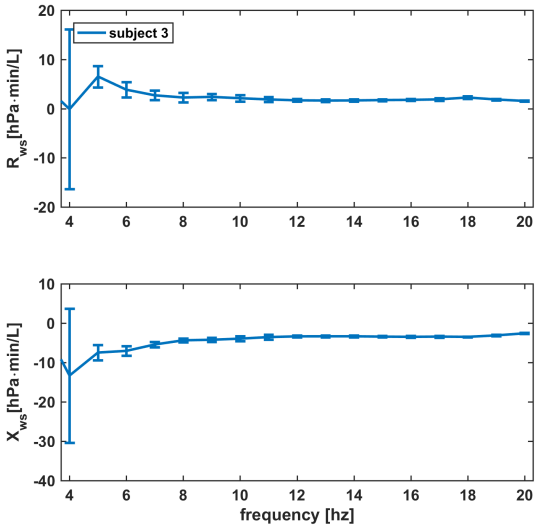

Figure D.21: Resistance, reactance and their 95% confidence intervals of frequency sweep in subject 3 at 10 hPa of mean IAP.

4.2. Pressure sweeps

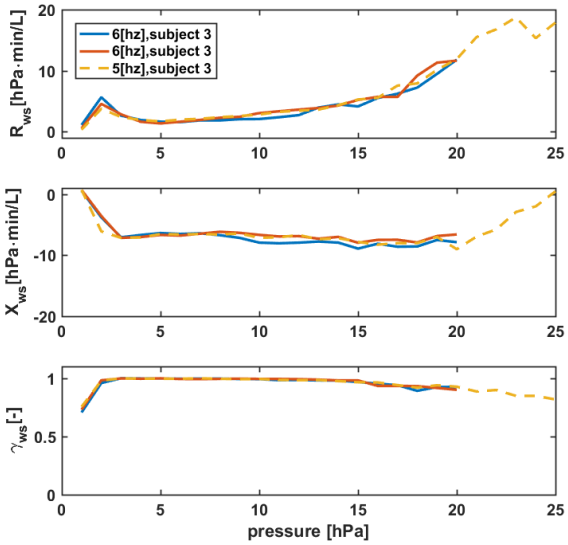

Figure D.22: Resistance, reactance and coherence during pressure sweeps in subject 3 at 6 Hz.

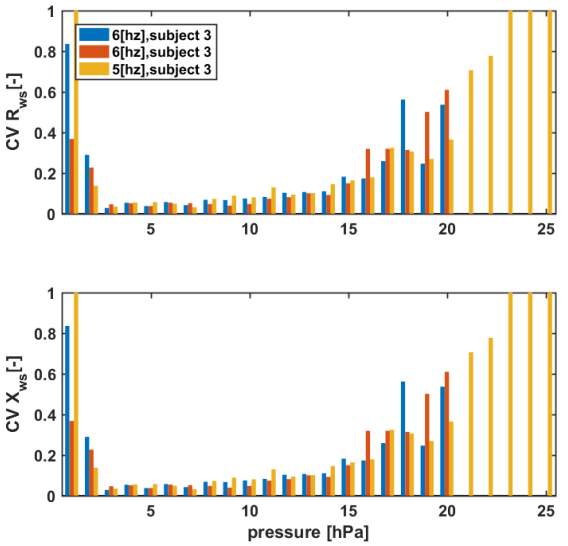

Figure D.23: Coefficients of variation in pressure sweeps in subject 3 at 6 Hz.

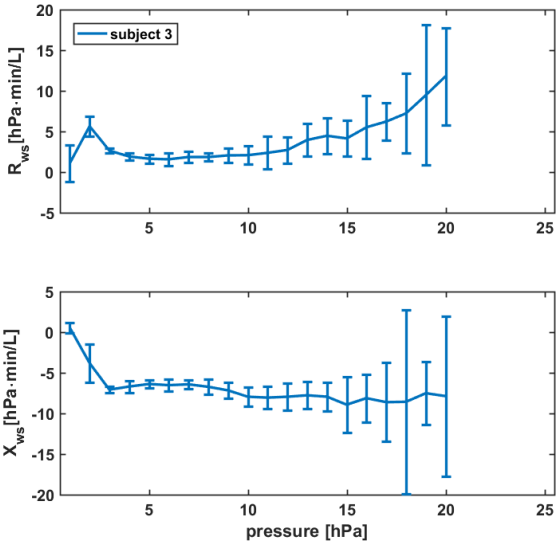

Figure D.24: Resistance, reactance and confidence intervals during pressure sweep in subject 3 at 6 Hz.

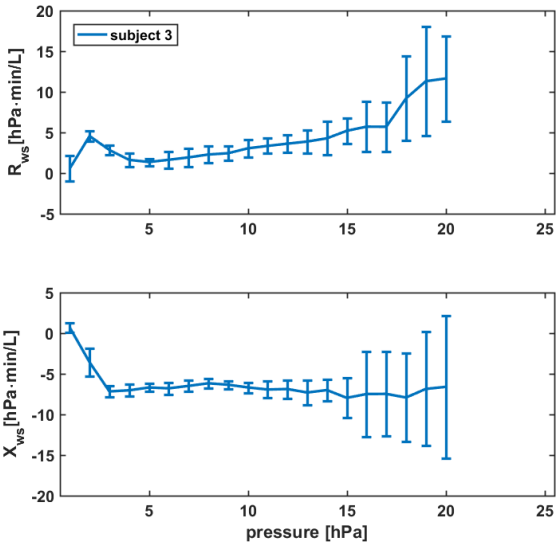

Figure D.25: Resistance, reactance and confidence intervals during pressure sweep in subject 3 at 6 Hz.

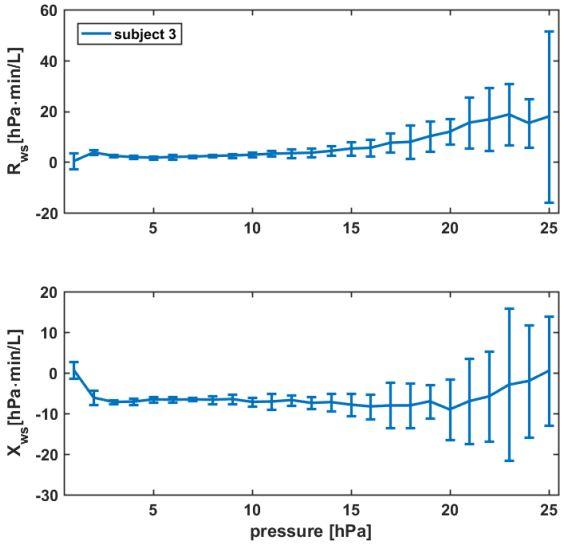

Figure D.26: Resistance, reactance and confidence intervals during extended pressure sweep in subject 3 at 6 Hz.

5. Subject #04, in-vivo

5.1. Frequency sweeps

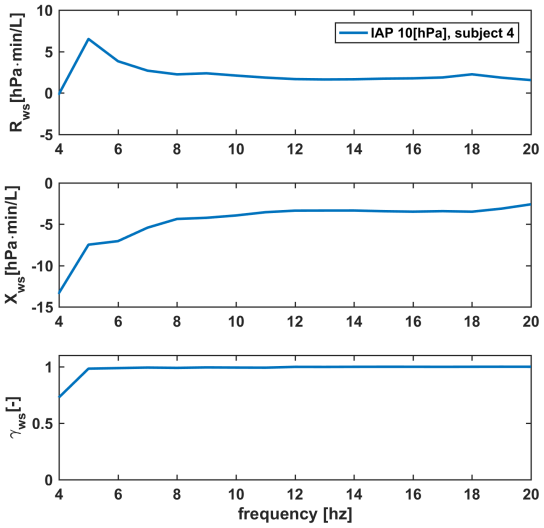

Figure D.27: Resistance, reactance and coherence during frequency sweeps in subject 4 at 5 and 10 hPa of mean IAP.

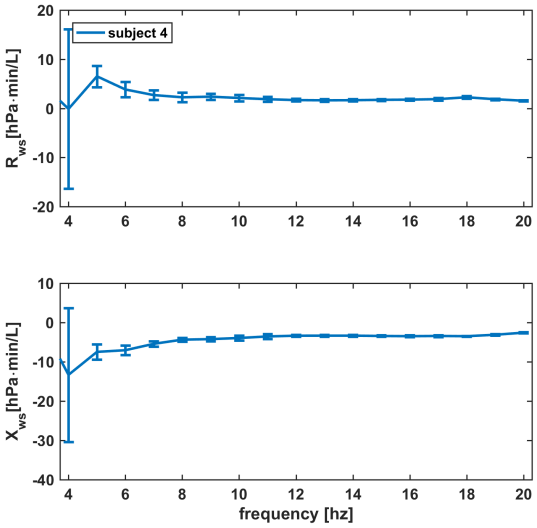

Figure D.29: Resistance, reactance and their 95% confidence intervals of frequency sweep in subject 4 at 5 hPa of mean IAP.

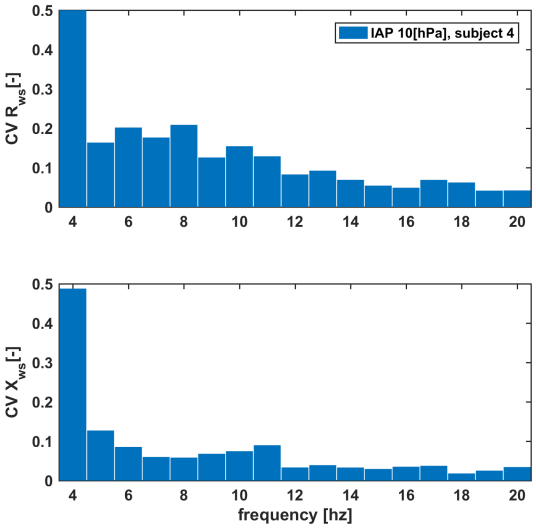

Figure D.28: Coefficients of variation in frequency sweeps in subject 4 at 5 and 10 hPa of mean IAP.

5.2. Pressure sweeps

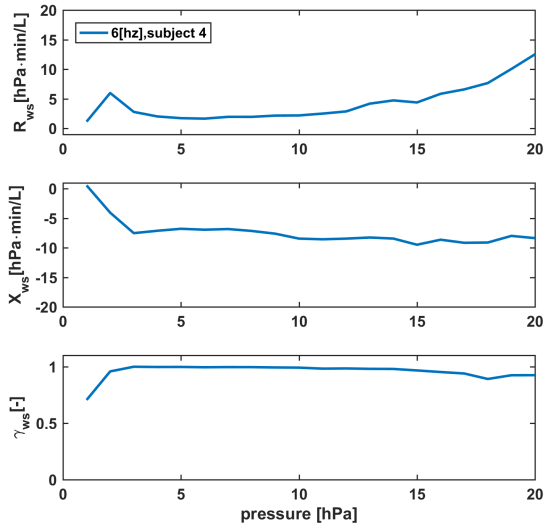

Figure D.30: Resistance, reactance and coherence during pressure sweeps in subject 4 at 6 Hz.

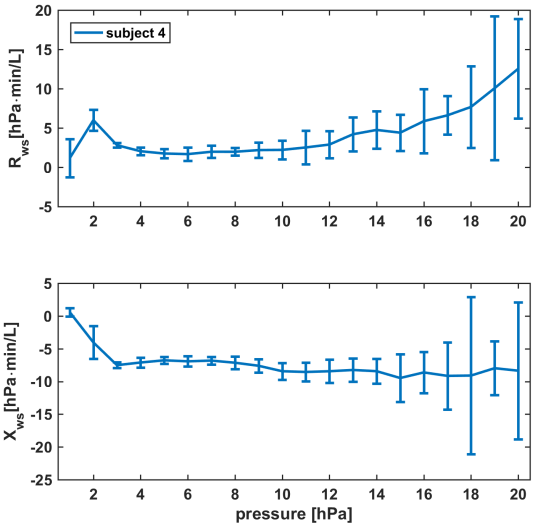

Figure D.32: Resistance, reactance and confidence intervals during pressure sweep in subject 4 at 6 Hz.

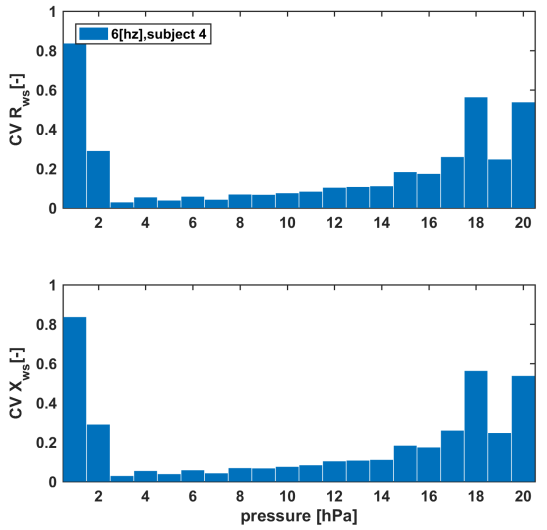

Figure D.31: Coefficients of variation in pressure sweeps in subject 4 at 6 Hz.